Note

Successful Colistin Treatment of Multidrug-Resistant *Pseudomonas aeruginosa* Infection Using a Rapid Method for Determination of Colistin in Plasma: Usefulness of Therapeutic Drug Monitoring

Takehiro Yamada,[a,b] Nobuhisa Ishiguro,[b] Kenji Oku,[c] Issei Higuchi,[a] Ikuma Nakagawa,[c] Atsushi Noguchi,[c] Shinsuke Yasuda,[c] Tatsuya Fukumoto,[b] Sumio Iwasaki,[b] Kouji Akizawa,[a] Ayako Furugen,[a] Hiroaki Yamaguchi,[a] and Ken Iseki*[,a,d]

[a] *Department of Pharmacy, Hokkaido University Hospital; Kita 14, Nishi 5, Kita-ku, Sapporo 060–8648, Japan:* [b] *Infection Control Team, Hokkaido University; Kita 14, Nishi 5, Kita-ku, Sapporo 060–8648, Japan:* [c] *Division of Rheumatology, Endocrinology, and Nephrology, Hokkaido University Graduate School of Medicine; Kita 15, Nishi 7, Kita-ku, Sapporo 060–8638, Japan: and* [d] *Laboratory of Clinical Pharmaceutics and Therapeutics, Division of Pharmasciences, Faculty of Pharmaceutical Sciences, Hokkaido University; Kita 12 Nishi 6, Kita-ku, Sapporo 060–0812, Japan.*

Received April 10, 2015; accepted June 23, 2015; advance publication released online July 9, 2015

A 56-year-old woman with systemic lupus erythematosus had bacteremia due to multidrug-resistant *Pseudomonas aeruginosa* (MDRP). She was initially treated with imipenem–cilastatin, tobramycin, and aztreonam; however, MDRP was still detected intermittently in her plasma. Multidrug-susceptibility tests demonstrated that MDRP was susceptible only to colistin. Therefore, in addition to these antibiotics, the administration of intravenous colistin methanesulfonate, a prodrug formula of colistin, was started at a daily dose of 2.5 mg/kg (as colistin base activity). The initial dose setting was based on the patient's renal function (baseline creatinine clearance=32.7 mL/min). After initiating colistin, the patient's C-reactive protein levels gradually decreased. Blood cultures showed no evidence of MDRP on days 8, 14, and 22 after colistin initiation. However, the patient's renal function went from bad to worse owing to septic shock induced by methicillin-resistant *Staphylococcus aureus* (MRSA) infection. A few days later, the trough plasma levels of colistin were 7.88 mg/L, which appeared to be higher than expected. After decreasing the colistin dose, the patient's renal function gradually improved. On the final day of colistin treatment, the plasma levels decreased to 0.60 mg/L. MDRP could not be detected in blood culture after colistin treatment. Therefore, we successfully treated a case of bloodstream infection due to MDRP by therapeutic drug monitoring (TDM) of colistin. It is suggested that the monitoring of blood colistin levels by liquid chromatography-tandem mass spectrometry can contribute to safer, more effective antimicrobial therapy of MDRP because TDM facilitates quick decisions on dose adjustments.

Key words colistin; drug monitoring; multidrug-resistant *Pseudomonas aeruginosa*

Colistin, known as an "old" antibiotic, has recently been reintroduced in clinical practice[1–3] because of the increased emergence of infections caused by multidrug-resistant Gram-negative bacteria.[2,4] Colistin was originally developed in Japan in the 1940s–1950s; however, initial studies reported adverse reactions, including nephrotoxicity or peripheral nervous system disorders.[5] Because of these adverse events and the introduction of safer antibiotics, clinical use of colistin was abandoned in Japan in 1990.

On the other hand, some reports have indicated the usefulness of colistin against multidrug-resistant *Pseudomonas aeruginosa* (MDRP) infection.[2,3]

Therapeutic drug monitoring (TDM) is a method used for determining the blood concentrations of drugs and optimizing the dose. Although a few case reports[6,7] have been published on TDM of colistin, these data were retrospectively determined after the end of treatment. To the best of our knowledge, this is the first report on a case in which TDM-based dosing optimization of colistin was applied to treat an MDRP bloodstream infection.

As for the determination method of drug level, traditional determination systems using high-performance liquid chromatography (HPLC) require time-consuming sample pretreatment such as solid phase extraction and derivatization of colistin because of its poor UV absorption and no native fluorescence.[8,9] For the detection of colistin level in blood, we utilized liquid chromatography-tandem mass spectrometry (LC-MS/MS), a widely used technology for determination of drug concentrations because of its high sensitivity and selectivity, which enabled us to monitor and maintain optimal blood colistin levels. The retention time of colistin on HPLC and LC-MS/MS is 15 min[9] and 3 min, respectively. Furthermore, it requires relatively little time to detect colistin. Prompt monitoring to ensure appropriate plasma colistin levels will contribute to more favorable treatment because patients suffering from MDRP infections are at a risk of rapid deterioration and thus require early treatment. Here we report a case in which colistin dose was carefully adjusted using TDM.

PATIENTS AND METHODS

Plasma Colistin Determination Plasma colistin levels were determined using LC-MS/MS using the method reported by Jansson *et al.*[10] with slight modification. In brief, 180 μL of plasma was spiked with 20 μL of colistin working solution (100, 50, 25, 12.5, and 0 mg/L), and polymyxin B was used as

* To whom correspondence should be addressed. e-mail: ken-i@pharm.hokudai.ac.jp

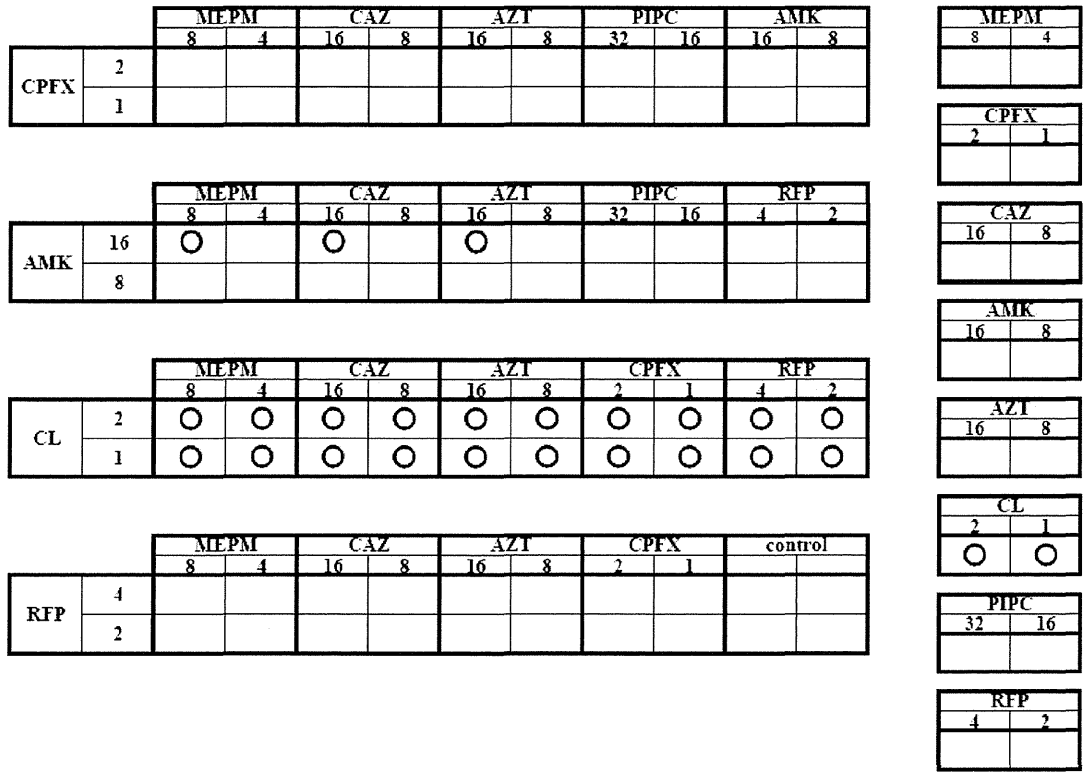

Fig. 1. Investigation of the Synergistic Effects of Antibiotics with Colistin Using the Breakpoint Checkerboard Plate

This assay is usually performed to evaluate the *in vitro* effects of the combination of multiple antibiotics against isolated MDRP in blood from this patient. Numbers mean concentration (mg/L) of each antibiotics which showed inhibitory effects against isolated strain. MEPM, meropenem; CAZ, ceftazidime; AZT, aztreonam; PIPC, piperacillin; AMK, amikacin; RFP, rifampicin; CPFX, ciprofloxacin; CL, colistin.

the internal standard. The samples were mixed with equal volumes of 0.1% trifluoroacetic acid in acetonitrile. After centrifugation at 15000 rpm for 15 min, the supernatant was mixed with an equal volume of 0.03% trifluoroacetic acid in water. Aliquots of the mixture (30 μL) were applied to LC-MS/MS.

Ethics The present study was carried out in accordance with the guidelines for the care for human study, and the study protocol was approved by the ethics committee of the Hokkaido University Hospital.

CASE REPORT

A 56-year-old woman (body height, 150 cm and weight, 61.4 kg) with systemic lupus erythematosus had bacteremia due to MDRP. She had been treated with imipenem–cilastatin (IPM/CS; 500 mg, twice daily) against extended-spectrum beta-lactamase-producing *Krebsiella pneumoniae*, tobramycin (TOB; 2 mg/kg, every 48 h), which was the only sensitive antibiotic for initially detected *Pseudomonas aeruginosa*, and aztreonam (AZT; 1000 mg, twice daily) for 57 d; however, MDRP was still detected in blood intermittently. On the other hands, before detection in blood culture, MDRP was detected in a urine sample (62 d before the start of colistin treatment), and the patient presented with pyelonephritis due to the bacterial infection. Thus, the source of infection was thought to be from urinary tract in this case. Multidrug susceptibility tests using the breakpoint checkerboard plate method demonstrated that MDRP was susceptible only to colistin, whose minimum inhibitory concentration against MDRP was equal to or less than 1 mg/L (Fig. 1). Therefore, in addition to AZT, intravenous colistin (as a prodrug formula) was initiated at a daily dose of 2.5 mg/kg (as colistin base activity, Fig. 2). The initial dose setting of colistin was based on the guidelines of the Japanese Society of Chemotherapy for the appropriate use of colistin (released on July 2012). Prior to the administration of colistin, *N*-acetyl-β-D-glucosaminidase (NAG) levels in urine were 39.4 U/L and the urinary creatinine-adjusted value (NAG/Cre) was 158. Eight days after starting colistin, NAG and NAG/Cre levels were markedly elevated to 75.3 U/L and 290, respectively (Fig. 3). On the first day of colistin administration, serum creatinine levels and creatinine clearance (CCr, calculated using the Cockcroft–Gault equation) were 1.86 mg/dL and 32.7 mL/min, respectively. Until day 14 after initiating colistin, serum creatinine levels increased gradually to 2.77 mg/dL and CCr was 23.6 mL/min. On day 13, the trough levels of colistin were found to be higher (7.88 mg/L) than expected[1] (Fig. 3). Therefore, the daily dosage of colistin was decreased to 1.5 mg/kg; however, the patient's serum creatinine levels remained high for approximately 48 h, after which her renal function recovered, showing serum creatinine levels of 1.36 mg/dL on the day after decreasing colistin dosage (day 20, Fig. 2). On days 8, 14 and 22 after initiating colistin, MDRP could not be detected in her blood. Moreover, MDRP could not be detected in the blood culture even one week after the end of colistin treatment. Colistin was continued for 21 d and the C-reactive protein (CRP) levels markedly decreased from 13.75 to 2.47 mg/dL. Overall, the colistin treatment was clinically and bacteriologically effective. Meanwhile, 10 d

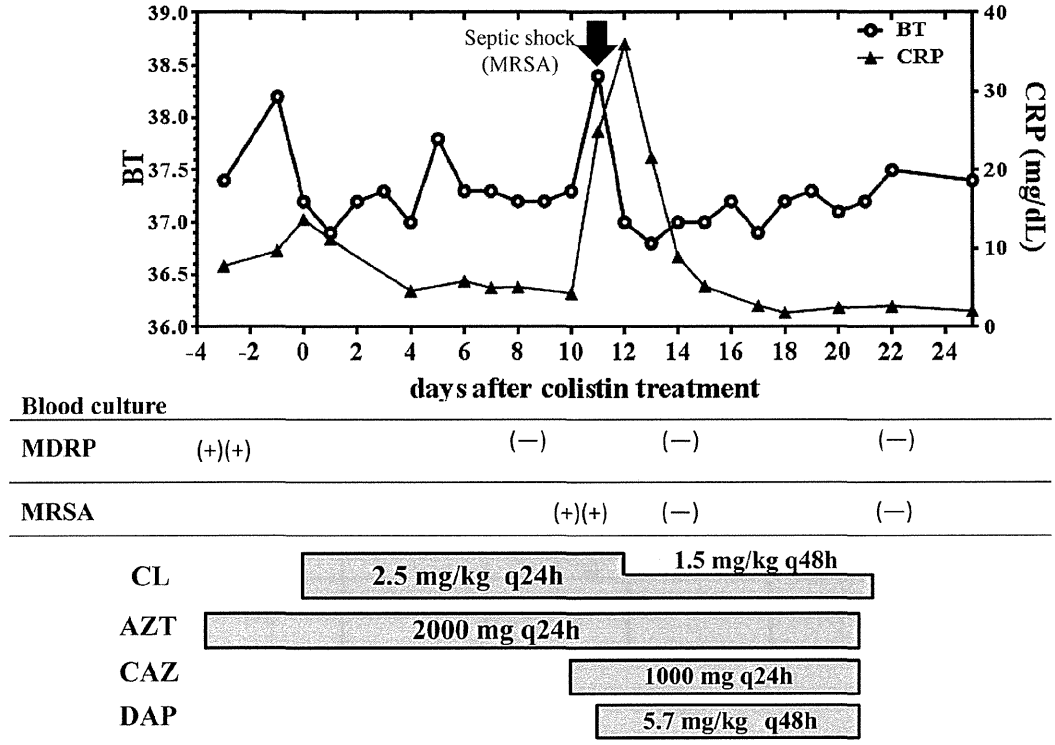

Fig. 2. Clinical Course of This Case

Colistin was initiated against blood-stream infection of MDRP. After starting colistin, MDRP in blood was disappeared on the day 8. Although this patient fell into septic shock evoked by MRSA infection (day 11, arrow), which was improved after starting daptomycin (DAP). BT, body temperature; CRP, C-reactive protein.

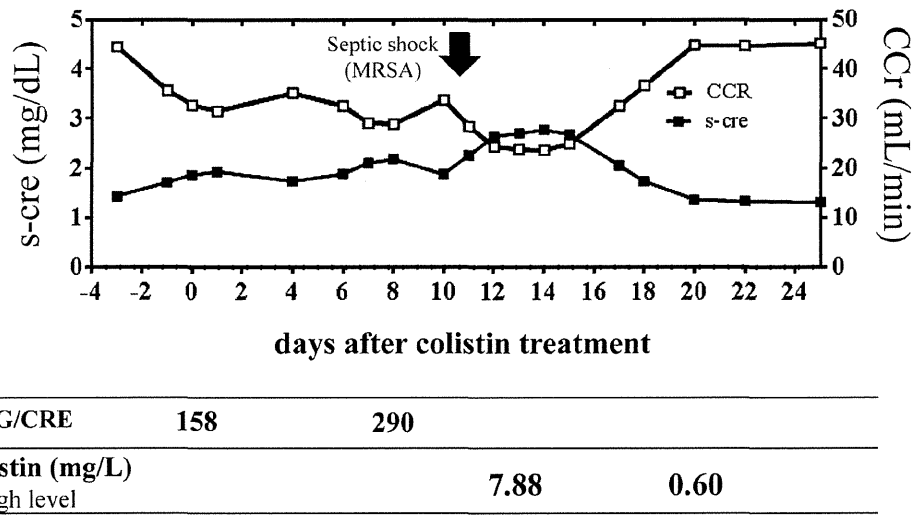

Fig. 3. Change of Renal Function and Plasma Colistin Level during the Antimicrobial Treatment

Renal function got worse after MRSA-evoked septic shock (day 11, arrow). NAG, *N*-acetyl-*β*-D-glucosaminidase; CRE, creatinine; s-cre, serum creatinine; CCr, creatinine clearance.

after starting colistin, the patient fell into septic shock owing to methicillin-resistant *Staphylococcus aureus* (MRSA) infection. A subcutaneous abscess caused by MRSA under the sutured wound because of the aortic valve replacement after developing congestive heart failure was thought to be the source of MRSA sepsis. On this day, ceftazidime was started for the reinforcement of the treatment against the Gram-negative bacterial infection. After starting daptomycin (DAP), CRP and BT levels decreased markedly (Fig. 2). On the last day of colistin treatment, her BT and CRP levels had improved and her renal function recovered to nearly normal levels.

DISCUSSION

The emergence of MDRP is becoming one of the major clinical issues in nosocomial infections, particularly in criti-

cally ill patients. Colistin is considered the first line drug for MDRP but has not yet been approved in Japan. We therefore obtained a parenteral formula of colistin [as the prodrug colistin methanesulfonate (CMS)] from a pharmaceutical company outside Japan. Recently, Mizuyachi *et al.*[11] reported the pharmacokinetic profiles of colistin and CMS in healthy Japanese male subjects, and Couet *et al.*[12] reported the results in healthy Caucasian subjects. The plasma half-life ($t_{1/2}$) of colistin is estimated to be approximately 3 h. However, in a study of critically ill patients, $t_{1/2}$ of colistin was prolonged up to 14.4 h.[1] In the previous study, a strong inverse trend was observed between steady-state plasma colistin levels and creatinine clearance. Thus, renal dosage and interval adjustment in colistin treatment are required, particularly for patients with kidney dysfunction.

A prospective observational cohort study demonstrated that trough plasma levels of colistin is an independent risk factor for nephrotoxicity[13] and that trough plasma colistin levels of 3.33 mg/L on day 7 best predicted acute kidney injury (AKI). Information on the plasma levels of colistin will be helpful for future dosing recommendations. To promptly determine the colistin trough level, we utilized a new method based on LC-MS/MS without time-consuming preparation. We experienced trough colistin levels as high as 7.88 mg/L on day 13 after starting colistin treatment. The patient's renal function tended to worsen, with creatinine clearance decreasing to 23.8 mL/min because of sepsis evoked by MRSA bloodstream infection; however, this transient renal dysfunction may have been partly due to colistin.

From day 14 after initiation of DAP for MRSA-induced sepsis, the patient's renal function recovered gradually. On day 20 after starting colistin treatment, plasma colistin levels were decreased by 0.61 mg/L; this decline was thought to be due to the recovery of her creatinine clearance.

If the plasma levels of colistin are below the MIC value for a very large proportion of the dosage interval, there is a possibility that the treatment has failed.[8] In the present case, MDRP in the blood culture was negative even one week after the end of colistin treatment. Her CRP level was remained lower than that on the day of starting colistin treatment, suggesting bacteriological and clinical effectiveness of colistin in this case. In addition, although the NAG/CRE value was examined only 2 points (Fig. 2), her daily urinary volume recovered to normal level (day 13 of colistin treatment, 150 mL, day 20, 2200 mL) after decreasing the colistin daily dose, suggesting that dose optimization of colistin is effective. These effects were due to TDM-based dosing of colistin, which contribute to avoid worsening of the renal function. Thus, TDM-based dosing of colistin is beneficial for patient safety. We were able to use colistin in a safer and more effective manner with TDM than without it. TDM-based colistin therapy will be a strong method for the patients suffering from MDRP.

Conflict of Interest The authors declare no conflict of interest.

REFERENCES

1) Garonzik SM, Li J, Thamlikitkul V, Paterson DL, Shoham S, Jacob J, Silveira FP, Forrest A, Nation RL. Population pharmacokinetics of colistin methanesulfonate and formed colistin in critically ill patients from a multicenter study provide dosing suggestions for various categories of patients. *Antimicrob. Agents Chemother.*, **55**, 3284–3294 (2011).
2) Li J, Nation RL, Turnidge JD, Milne RW, Coulthard K, Rayner CR, Paterson DL. Colistin: the re-emerging antibiotic for multidrug-resistant Gram-negative bacterial infections. *Lancet Infect. Dis.*, **6**, 589–601 (2006).
3) Martis N, Leroy S, Blanc V. Colistin in multi-drug resistant *Pseudomonas aeruginosa* blood-stream infections: a narrative review for the clinician. *J. Infect.*, **69**, 1–12 (2014).
4) Montero M, Horcajada JP, Sorli L, Alvarez-Lerma F, Grau S, Riu M, Sala M, Knobel H. Effectiveness and safety of colistin for the treatment of multidrug-resistant *Pseudomonas aeruginosa* infections. *Infection*, **37**, 461–465 (2009).
5) Falagas ME, Kasiakou SK, Saravolatz LD. Colistin: the revival of polymyxins for management of multidrug-resistant Gram-negative bacterial infections. *Clin. Infect. Dis.*, **40**, 1333–1341 (2005). Corrected in *Clin. Infect. Dis.* in 2006, **42**, 1819.
6) Yaita K, Sameshima I, Takeyama H, Matsuyama S, Nagahara C, Hashiguchi R, Moronaga Y, Tottori N, Komatsu M, Oshiro Y, Yamaguchi Y. Liver abscess caused by multidrug-resistant *Pseudomonas aeruginosa* treated with colistin; a case report and review of the literature. *Intern. Med.*, **52**, 1407–1412 (2013).
7) Bode-Böger SM, Schopp B, Tröger U, Martens-Lobenhoffer J, Kalousis K, Mailänder P. Intravenous colistin in a patient with serious burns and borderline syndrome: the benefits of therapeutic drug monitoring. *Int. J. Antimicrob. Agents*, **42**, 357–360 (2013).
8) Li J, Coulthard K, Milne R, Nation RL, Conway S, Peckham D, Etherington C, Turnidge J. Steady-state pharmacokinetics of intravenous colistin methanesulphonate in patients with cystic fibrosis. *J. Antimicrob. Chemother.*, **52**, 987–992 (2003).
9) Li J, Milne RW, Nation RL, Turnidge JD, Coulthard K, Valentine J. Simple method for assaying colistin methanesulfonate in plasma and urine using high-performance liquid chromatography. *Antimicrob. Agents Chemother.*, **46**, 3304–3307 (2002).
10) Jansson B, Karvanen M, Cars O, Plachouras D, Friberg LE. Quantitative analysis of colistin A and colistin B in plasma and culture medium using a simple precipitation step followed by LC-MS/MS. *J. Pharm. Biomed. Anal.*, **49**, 760–767 (2009).
11) Mizuyachi K, Hara K, Wakamatsu A, Nohda S, Hirama T. Safety and pharmacokinetic evaluation of intravenous colistin methansulfonate sodium in Japanese healthy male subjects. *Curr. Med. Res. Opin.*, **27**, 2261–2270 (2011). Corrected in *Curr. Med. Res. Opin.*, 2015, **31**, 593–594.
12) Couet W, Gregoire N, Gobin P, Saulnier PJ, Frasca D, Marchand S, Mimoz O. Pharmacokinetics of colistin and colistimethate sodium after a single 80-mg intravenous dose of CMS in young healthy volunteers. *Clin. Pharmacol. Ther.*, **89**, 875–879 (2011).
13) Sorli L, Luque S, Grau S, Berenguer N, Segura C, Montero MM, Álvarez-Lerma F, Knobel H, Benito N, Horcajada JP. Trough colistin plasma level is an independent risk factor for nephrotoxicity: a prospective observational cohort study. *BMC Infect. Dis.*, **13**, 380 (2013).

The American Journal of Pathology, Vol. 186, No. 1, January 2016

ELSEVIER

The American Journal of
PATHOLOGY

ajp.amjpathol.org

EPITHELIAL AND MESENCHYMAL CELL BIOLOGY

Platelets Regulate the Migration of Keratinocytes via Podoplanin/CLEC-2 Signaling during Cutaneous Wound Healing in Mice

Jun Asai,* Satoshi Hirakawa,† Jun-ichi Sakabe,† Tsunao Kishida,† Makoto Wada,* Naomi Nakamura,* Hideya Takenaka,* Osam Mazda,‡ Tetsumei Urano,§ Katsue Suzuki-Inoue,¶ Yoshiki Tokura,† and Norito Katoh*

From the Departments of Dermatology and Immunology,‡ Kyoto Prefectural University of Medicine, Kyoto; the Departments of Dermatology† and Physiology,§ Hamamatsu University School of Medicine, Hamamatsu; and the Department of Clinical and Laboratory Medicine,¶ Faculty of Medicine, University of Yamanashi, Kofu, Japan*

Accepted for publication September 24, 2015.

Address correspondence to Jun Asai, M.D., Ph.D., Department of Dermatology, Kyoto Prefectural University of Medicine, 465 Hirokoji, Kawaramachi, Kamigyo-Ku, Kyoto 602-8566, Japan. E-mail: jasai@koto.kpu-m.ac.jp.

Podoplanin is an endogenous ligand for C-type lectin-like receptor 2 (CLEC-2), which is expressed on platelets. Recent evidence indicates that this specific marker of lymphatic endothelial cells is also expressed by keratinocytes at the edge of wounds. However, whether podoplanin or platelets play a role in keratinocyte activity during wound healing remains unknown. We evaluated the effect of podoplanin expression levels on keratinocyte motility using cultured primary normal human epidermal keratinocytes (NHEKs). Down-regulation of podoplanin in NHEKs via transfection with podoplanin siRNA inhibited their migration, indicating that podoplanin plays a mandatory role in this process. In addition, down-regulation of podoplanin was correlated with up-regulation of E-cadherin, suggesting that podoplanin-mediated stimulation of keratinocyte migration is associated with a loss of E-cadherin. Both the addition of platelets and treatment with CLEC-2 inhibited the migration of NHEKs. The down-regulation of RhoA activity and the up-regulation of E-cadherin in keratinocytes were also induced by CLEC-2. In conclusion, these results suggest that podoplanin/CLEC-2 signaling regulates keratinocyte migration via modulating E-cadherin expression through RhoA signaling. Altering the regulation of keratinocyte migration by podoplanin might be a novel therapeutic approach to improve wound healing. *(Am J Pathol 2016, 186: 101–108; http://dx.doi.org/10.1016/j.ajpath.2015.09.007)*

Podoplanin, a small 38-kDa mucin-type transmembrane glycoprotein, is expressed in kidney podocytes (the origin of its nomenclature), type I lung alveolar epithelial cells, and lymphatic endothelial cells.[1,2] Recently, podoplanin has been implicated in tumor progression.[3–6] Podoplanin expression is up-regulated in the invasive front of several human carcinomas, including squamous cell carcinomas of the oral cavity, lung, and skin.[7,8] The expression of this glycoprotein is correlated with the down-regulation of the cell-cell adhesion protein E-cadherin,[9] which leads to tumor invasion via stimulation of the epithelial-mesenchymal transition. In addition to tumor cells, epidermal keratinocytes express podoplanin under several pathological conditions, such as wound healing and psoriasis.[10,11] However, the role of podoplanin in normal epidermal keratinocytes during wound healing remains unknown.

C-type lectin-like receptor 2 (CLEC-2) is a receptor for the platelet-activating snake venom, rhodocytin.[12] Podoplanin was identified as an endogenous ligand for CLEC-2[13] and induces platelet aggregation by binding to CLEC-2. This contributes to thrombosis/hemostasis, lymphangiogenesis, and tumor metastasis.[13,14] During wound healing processes, platelet aggregation and clot formation are the initial steps of tissue regeneration. Platelet-rich aggregates release various growth factors and cytokines to promote wound healing. Platelet lysates stimulate the proliferation and migration of immortalized HaCaT keratinocytes,[15] although this cell line does not express podoplanin.[16] However, the physiological significance of

Supported by JSPS KAKENHI grant 25461674 (J.A.).
Disclosures: None declared.

http://dx.doi.org/10.1016/j.ajpath.2015.09.007

the podoplanin/CLEC-2 interaction between platelets and normal keratinocytes remains to be investigated.

Herein, we investigated the function of podoplanin in normal keratinocytes, with special focus on the alterations in motility induced by podoplanin siRNA and the interaction between platelets and keratinocytes. The results suggest that podoplanin plays a mandatory role in keratinocyte migration and that platelets inhibit the migration of keratinocytes. We further determined that the regulatory effects of platelets on keratinocytes were mediated by podoplanin/CLEC-2 signaling.

Materials and Methods

Wound Induction

Male C57BL/6 mice used in this study were between 8 and 10 weeks of age at the time of the study. Wounds were induced as described previously.[17–20] In brief, after induction of deep anesthesia by i.p. injection of 160 mg/kg sodium pentobarbital, full-thickness excisional skin wounds were made on the backs of mice using 8-mm skin biopsy punches, with one wound generated in each mouse. Each wound was covered with semipermeable polyurethane dressing (OpSite; Smith and Nephew, Massillon, OH). Wound tissues were harvested on days 1, 3, 7, and 10 after wound induction. All animal protocols were approved by the Kyoto Prefectural University of Medicine (Kyoto, Japan) Institutional Animal Care and Use Committee, and were consistent with the *Guide for the Care and Use of Laboratory Animals*.[21]

Cell Culture

Primary normal human epidermal keratinocytes (NHEKs; Kurabo, Osaka, Japan) were cultured in HuMedia-KG2 serum-free medium (Kurabo).

Platelet Preparation

Venous blood from a healthy drug-free patient, who was scheduled to have plastic surgery, was collected into 10% sodium citrate at the time of their blood test. This study was approved by the Ethical Committee of the Kyoto Prefectural University of Medicine, and written informed consent was provided according to the Declaration of Helsinki. Platelets were obtained by centrifugation, as described previously, using prostacyclin to prevent activation during the isolation procedure.[22]

siRNA Transfection

Control or podoplanin siRNA (50 nmol/L; Hs[lowen]PDPN [lowen]1 FlexiTube siRNA, catalog number SI03060260; Qiagen, Düsseldorf, Germany) was transfected into NHEKs using Lipofectamine RNAiMAX (Invitrogen, Carlsbad, CA), according to the manufacturer's protocol. For RT-PCR

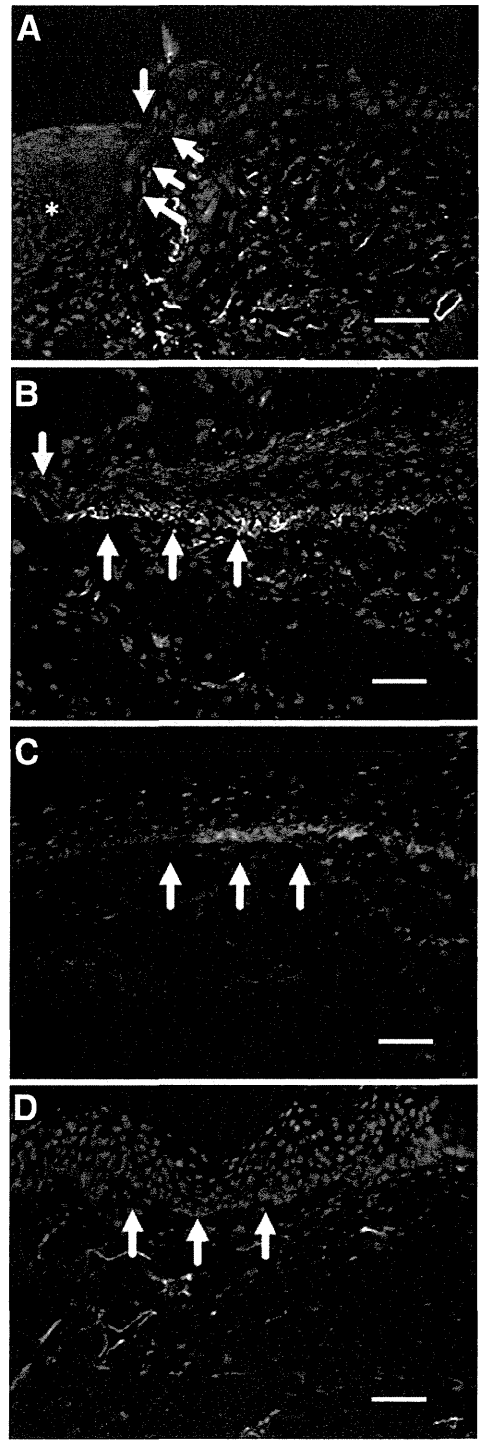

Figure 1 Time-dependent expression of podoplanin in keratinocytes during wound healing. Green and blue fluorescence corresponds to podoplanin-positive cells and DAPI-labeled nuclei, respectively. Wound edge during the inflammatory phase (day 1; **A**), during the tissue formation phase (day 3; **B**), at the period of transition from the tissue formation phase to the tissue remodeling phase (day 7; **C**), and at the end of the tissue remodeling phase (day 10; **D**). The **asterisk** indicates platelet aggregates covering the surface of the wound; **yellow arrows**, the leading edge of the epidermis; **white arrows**, the basal cell layer of the epidermis at the wound edge. Scale bars: 50 μm (**A–D**). Original magnification, ×100 (**A–D**).

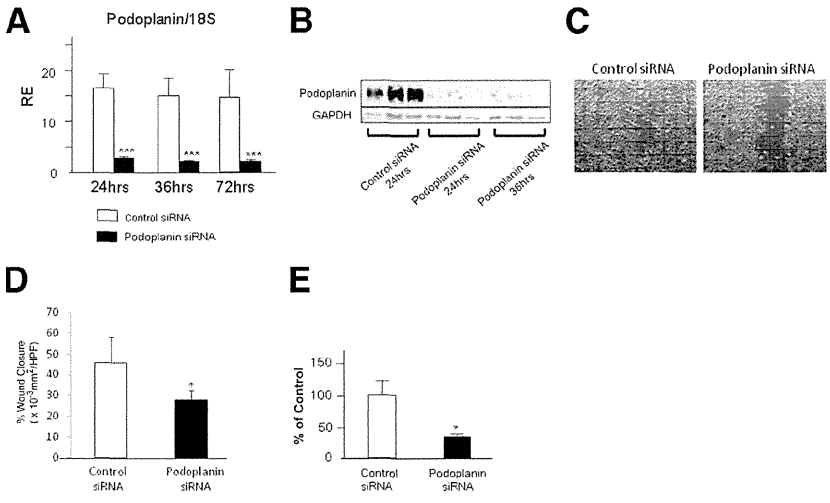

Figure 2 Efficacy of podoplanin siRNA in normal human epidermal keratinocytes (NHEKs). NHEKs were harvested 24, 36, and 72 hours after transfection. **A:** Quantitative RT-PCR of podoplanin mRNA in NHEKs treated with control or podoplanin siRNA. **B:** Western blot analysis of podoplanin protein expression in NHEKs treated with control or podoplanin siRNA. **C:** The effects of podoplanin down-regulation on NHEK migration. The migration of NHEKs transfected with control or podoplanin siRNA was investigated by the scratch wound assay. **D:** Graphical presentation of the wound closure areas, quantified as described in *Materials and Methods*. **E:** RhoA activity of NHEKs measured by the Great Lakes Integrated Sciences + Assessments Center assay. Control or podoplanin siRNA transfected cells were harvested at 24 hours after transfection. $*P < 0.05$, $***P < 0.001$ versus control siRNA. $n = 6$ in each group (**A** and **D**); $n = 3$ in each group (**B** and **E**). GAPDH, glyceraldehyde-3-phosphate dehydrogenase; HPF, high-power field; RE, relative expression.

and the scratch wound assay, cells were used 24 hours after transfection.

Immunofluorescence Staining

Sections of wounds were stained with a hamster anti-mouse podoplanin antibody (Angiobio, Del Mar, CA). Podoplanin labeling was visualized with a fluorescein-conjugated anti-hamster antibody (Vector Laboratories, Burlingame, CA). E-cadherin and N-cadherin expression was evaluated using goat anti-mouse E-cadherin and N-cadherin antibodies (R&D Systems, Minneapolis, MN), respectively, and a Cy3-conjugated anti-goat antibody (Vector Laboratories). Platelets were evaluated using a rat monoclonal anti-mouse CD41 antibody (AbD Serotec, Oxford, UK) labeled with a Cy3-conjugated anti-rat antibody (Vector Laboratories). NHEKs treated with 100 ng/mL CLEC-2 or vehicle for 72 hours were stained with a mouse polyclonal anti-human E-cadherin (R&D Systems), rabbit monoclonal β-catenin (Abcam, Cambridge, UK), or rabbit polyclonal N-cadherin (R&D Systems) antibody labeled with fluorescein isothiocyanate–conjugated anti-mouse or anti-rabbit antibodies (Vector Laboratories), as appropriate.

RNA Isolation, cDNA Synthesis, and Quantitative Real-Time PCR

RNA was extracted using ISOGENII (Nippon Gene, Toyama, Japan), according to the manufacturer's instructions, and processed for cDNA synthesis and quantitative RT-PCR, as previously described.[19] To evaluate the efficacy of podoplanin siRNA, NHEKs were harvested 24 and 36 hours after transfection. To evaluate the effects of platelets on NHEKs, NHEKs were harvested 24 hours after the addition of 2.0×10^5 platelets/mL. Recombinant human CLEC-2 (hCLEC-2; R&D Systems) was added to cultured NHEKs at the indicated concentrations, and cells were harvested after 24 hours. Podoplanin, E-cadherin, and N-cadherin mRNA levels were normalized on the basis of the level of 18S, an internal reference gene. The primers used in the study were obtained from Qiagen (podoplanin, catalog number QT01015084; E-cadherin, catalog number QT00080143; N-cadherin, catalog number QT00063196; 18S, catalog number QT00199367).

SDS-PAGE and Western Blot Analysis

Cells were lysed with radioimmunoprecipitation assay buffer (Invitrogen) and sonicated. After sonication, cell lysates were centrifuged at 13,000 × *g* for 20 minutes at 4°C, and the supernatants were collected into fresh tubes. We then added 4× SDS sample buffer with 0.1 mol/L dithiothreitol to each sample. Samples were heated for 5 minutes at 95°C, and 20 μg protein was separated by 10% SDS-PAGE and electroblotted onto polyvinylidene difluoride membranes for 2 hours at 180 mA. The membranes were incubated with a rabbit anti-human podoplanin polyclonal antibody (R&D Systems) or a mouse anti-glyceraldehyde-3-phosphate dehydrogenase monoclonal antibody (Santa Cruz Biotechnology, Dallas, TX) and detected with horseradish peroxidase–conjugated goat anti-rabbit IgG (Bio-Rad, Hercules, CA) or horseradish peroxidase–conjugated goat anti-mouse IgG (Bio-Rad). Immunoblots were visualized using an ECL Plus Western Blotting Detection Reagents Kit (GE Healthcare, Little Chalfont, Buckinghamshire, UK), according to the manufacturer's protocol.

Scratch Wound Assay

Scratch wounds were generated in confluent monolayers of NHEKs by using a 1-mL pipette tip. To evaluate the effects of podoplanin siRNA, NHEKs were used 24 hours after the

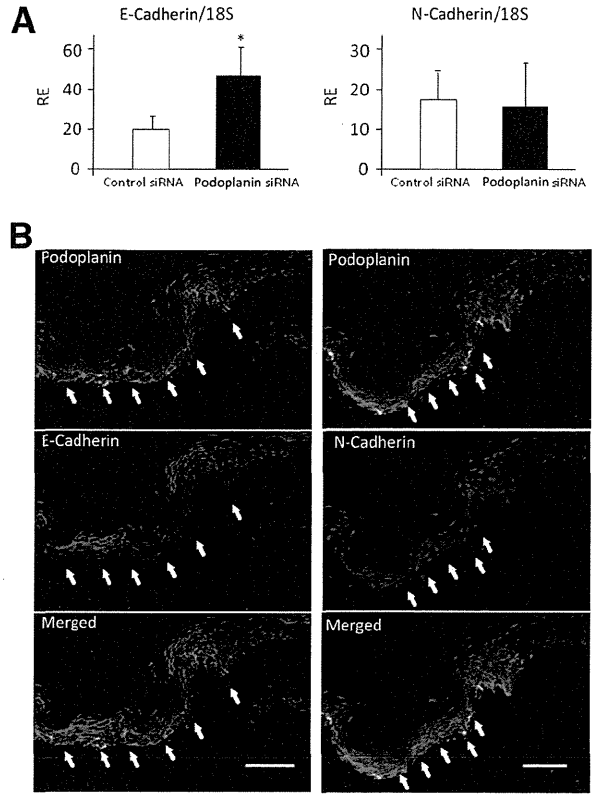

Figure 3 Cadherin expression in normal human epidermal keratinocytes (NHEKs) and keratinocytes at the wound edge. **A:** Quantitative RT-PCR of E-cadherin and N-cadherin mRNA in NHEKs transfected with control or podoplanin siRNA. **B:** Representative images of the immunostained wound edge at 3 days after wound generation. Red and green correspond to E-cadherin (**left panels**) or N-cadherin (**right panels**) and podoplanin, respectively. Blue fluorescence indicates DAPI-labeled nuclei. The **yellow arrows** indicate the leading edge of the epidermis; **white arrows**, basal cell layer of the epidermis at the wound edge. $^*P < 0.05$ versus control siRNA. $n = 6$ in each group (**A**). Scale bar = 50 μm (**B**). Original magnification, ×200 (**B**). RE, relative expression.

transfection. After washing away suspended cells, cultures were refed with medium. To evaluate the effects of platelets or CLEC-2 on NHEKs, 2.0×10^5 platelets/mL, or 10, 100, or 250 ng/mL hCLEC-2 was added to the NHEKs, respectively. Cell migration into the wound space was estimated at 18 hours after wounding. Images were analyzed using ImageJ software version 1.47v (NIH, Bethesda, MD; *http://imagej.nih.gov/ij*)[23] by tracing the wound margin with a high-resolution computer mouse and calculating the total pixel area.

Measurement of RhoA Activity

The direct activation of RhoA was evaluated using ELISA based small G-protein activation (G-LISA) assay (Cytoskeleton Inc., Denver, CO), according to the manufacturer's protocol. Briefly, NHEKs at 30% to 50% confluence, seeded onto 12-well flat-bottomed plates, were treated with 100 ng/mL CLEC-2. After incubation for 1, 5, 10, or 30 minutes at 37°C, cells were treated with lysis buffer. Rho-GTP in the cell lysate was detected using a RhoA G-LISA kit. The absorbance at 490 nm was recorded using a 96-well enzyme-linked immunosorbent assay plate reader.

Statistical Analysis

All results are presented as the means ± SEM. Statistical comparisons between two groups were performed by *t*-test. Multiple groups were analyzed by one-way analysis of variance, followed by appropriate post hoc tests to determine statistical significance. $P < 0.05$ was considered significant. All *in vitro* experiments were performed at least in triplicate.

Results

Expression of Podoplanin by Keratinocytes during Wound Healing

To evaluate the time-dependent expression of podoplanin during wound healing, full-thickness wounds were generated on the dorsal skin of mice (Figure 1). Podoplanin expression started to be observed at day 1, which represented the inflammatory phase in the wound healing process. Podoplanin expression was highly up-regulated at days 3 and 7 after

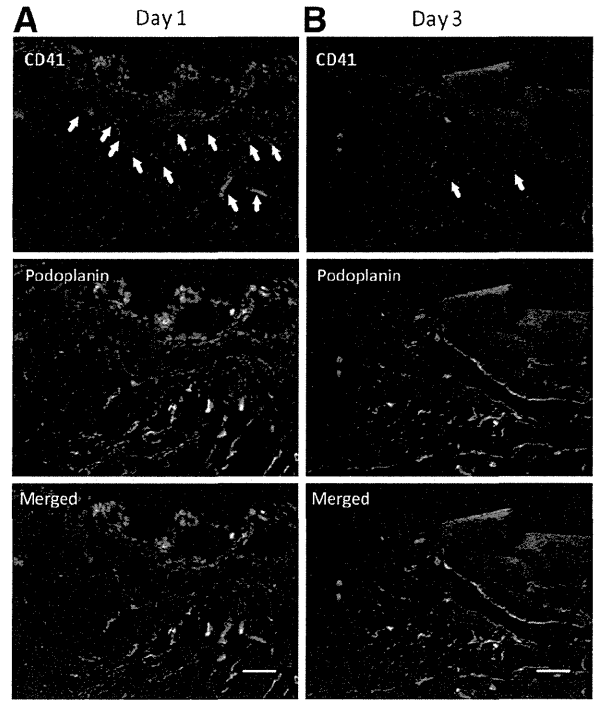

Figure 4 Direct interaction of platelets and keratinocytes during wound healing. Green, red, and blue fluorescence corresponds to podoplanin-positive cells, CD41-positive cells (platelets), and DAPI-labeled nuclei, respectively. Wound edge during the inflammatory phase (day 1; **A**) and during the tissue formation phase (day 3; **B**). **White arrows** indicate the accumulation of platelets on the basal cell layer of the epidermis at the wound edge. Scale bar = 50 μm (**A** and **B**). Original magnification, ×100 (**A** and **B**).

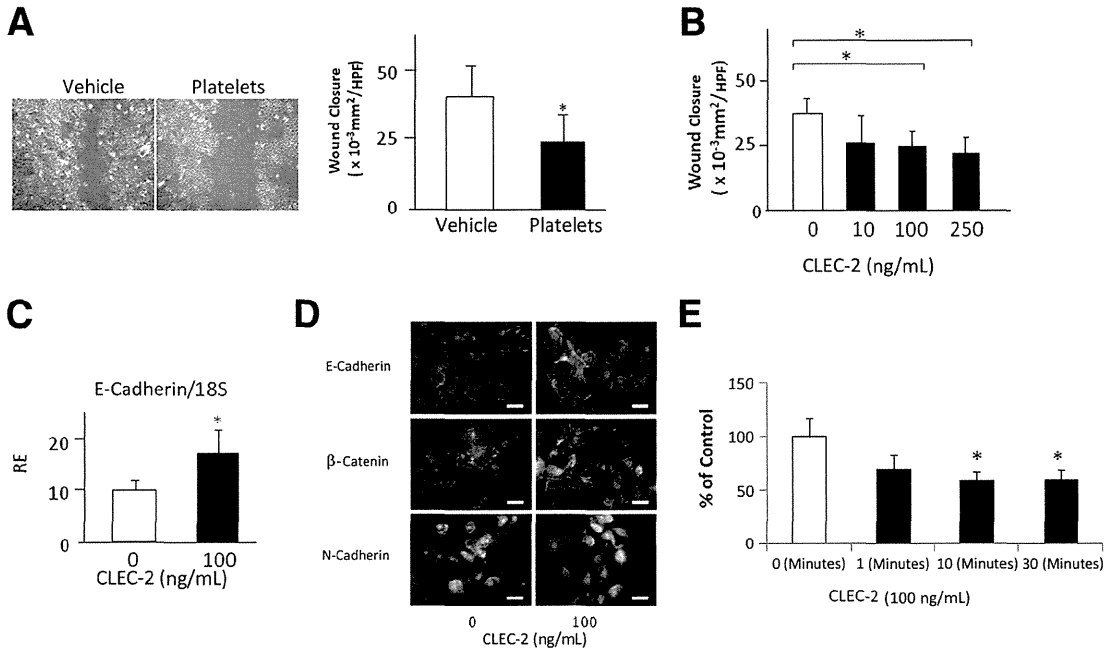

Figure 5 Effects of platelets on keratinocyte motility. **A:** Migration of normal human epidermal keratinocytes (NHEKs) treated with either 2.0×10^5 platelets/mL or vehicle was investigated by the scratch wound assay. Graphical presentation of the wound closure area, quantified as described in *Materials and Methods*. **B:** Graphical representation of the wound closure area after treatment with 10, 100, or 250 ng/mL human C-type lectin-like receptor 2 (hCLEC), or with vehicle, quantified as described in *Materials and Methods*. **C:** Quantitative RT-PCR of E-cadherin mRNA in NHEKs treated with 100 ng/mL hCLEC-2 or vehicle. **D:** Immunofluorescence staining of E-cadherin, β-catenin, and N-cadherin of NHEKs treated with 100 ng/mL CLEC-2. **E:** RhoA activity of NHEKs measured by the Great Lakes Integrated Sciences + Assessments Center assay. To each culture, 100 ng/mL hCLEC-2 was added, and cells were harvested at the indicated time point. $^*P < 0.05$ versus control siRNA. $n = 6$ in each group (**A–C**); $n = 3$ in each group (**E**). Scale bar = 50 μm (**D**). HPF, high-power field; RE, relative expression.

wounding, and it had decreased by day 10 when the wound was completely closed.

Effects of Podoplanin siRNA on NHEKs

To examine the efficacy of podoplanin siRNA, podoplanin mRNA and protein levels were analyzed by quantitative RT-PCR and Western blot analysis, respectively. Transfection of podoplanin siRNA into NHEKs resulted in significant decrements in both the mRNA (Figure 2A) and protein (Figure 2B) levels up to 72 and 36 hours after transfection, respectively, compared with those after transfection of the control siRNA ($P < 0.001$).

We next investigated the effects of down-regulating podoplanin on the motility of NHEKs using the scratch wound assay (Figure 2C). Twenty-four hours after transfection with podoplanin siRNA, a scratch wound was generated on a confluent monolayer of NHEKs and the non-cell area was measured. Eighteen hours after the scratch, the non-cell area was again measured. The wound closure area was analyzed by subtracting the latter from the former area. Podoplanin siRNA transfection significantly inhibited the migration of NHEKs by 40% (Figure 2D). To confirm that these results were induced specifically by podoplanin down-regulation, we performed the experiments using a different podoplanin siRNA (Hs[lowen]T1A-2[lowen]7, catalog S102625049; Qiagen) and obtained similar results (Supplemental Figure S1).

To evaluate the mechanisms of podoplanin-mediated cell motility, RhoA activity, which is one of the key mediators of cell migration, was directly measured by G-LISA. RhoA activity was down-regulated by podoplanin siRNA knockdown (Figure 2E), suggesting that podoplanin mediates keratinocyte motility partly via the RhoA signaling pathway.

Because the down-regulation of E-cadherin and the up-regulation of N-cadherin promote cell motility and the epithelial-mesenchymal transition in several tumor cells,[24] we next investigated the relationship between podoplanin and E- or N-cadherin in cultured NHEKs and epidermal keratinocytes at the wound edge. Down-regulation of podoplanin by siRNA significantly up-regulated the E-cadherin transcriptional level of NHEKs, whereas no significant change was observed in N-cadherin expression (Figure 3A). Similarly to the results in cultured NHEKs, podoplanin and E-cadherin expression showed inverse correlation in keratinocytes at the wound edge (Figure 3B). At the basal cell layer, keratinocytes showed strong expression of podoplanin and weak expression of E-cadherin, and at the upper layer, they exhibited weak podoplanin and strong E-cadherin expression. In addition, podoplanin and N-cadherin expression appeared to be mostly colocalized (Figure 3B).

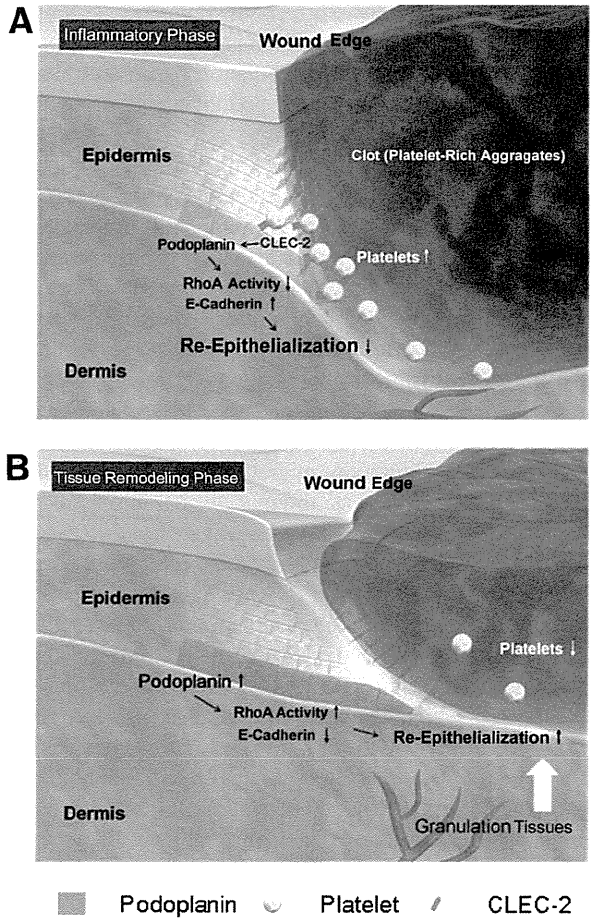

Figure 6 Potential functional mechanisms of platelets on wound healing. One of the important functions of platelets on wound healing is to delay re-epithelialization until wound bed preparation is completed. **A:** During the inflammatory phase, platelets inhibit re-epithelialization on the surface of immature granulation tissue by regulating podoplanin function via C-type lectin-like receptor 2 (CLEC-2). **B:** During the tissue formation to the remodeling phase, after platelet aggregates are replaced by granulation tissue and bleeding has stopped, the expression of podoplanin is up-regulated and re-epithelialization proceeds via RhoA activation and loss of E-cadherin.

Taken together, these results indicate that podoplanin down-regulation resulted in decreased NHEK migration with up-regulation of the cell-cell adhesion molecule, E-cadherin.

Effect of Platelets on NHEK Motility

Podoplanin is an endogenous ligand for CLEC-2[13] and induces platelet aggregation by binding to this receptor.[13,14] Therefore, we sought to determine the role of the podoplanin/CLEC-2 interaction in the effects of platelets on keratinocytes. First, we evaluated the direct adhesion of platelets onto keratinocytes by immunofluorescence staining (Figure 4). One day after wounding, which represents the inflammatory phase of the wound healing process, CD41-positive platelets were observed to be localized at the upper dermis and the basal layer of keratinocytes at the wound edge; podoplanin expression in keratinocytes was not clearly up-regulated. Three days after wounding, which represents the tissue formation phase, the localization of platelets on the upper dermis and the basal cell layer decreased and podoplanin expression in keratinocytes at the wound edge was markedly up-regulated. These findings provided evidence of functional interaction between platelets and keratinocytes. We next investigated the effects of platelets on the motility of NHEKs using the scratch wound assay. After generation of a scratch wound on confluent NHEKs using a pipette tip, 2.0×10^5 platelets/mL were added. Platelets significantly inhibited the migration of NHEKs by 40% (Figure 5A). To evaluate whether the interaction between podoplanin/CLEC-2 contributed to the inhibition of NHEK migration by platelets, 10, 100, or 250 ng/mL hCLEC-2 was added to the NHEK culture. The addition of hCLEC-2 inhibited the migration of NHEKs in a dose-dependent manner ($P < 0.05$) (Figure 5B) and up-regulated E-cadherin mRNA (Figure 5C). E-cadherin up-regulation was confirmed by immunofluorescence staining. The E-cadherin signal was strongly positive at the peripheral area of the NHEKs, whereas no significant change was observed in β-catenin and N-cadherin expression (Figure 5D).

Because RhoA is one of the key mediators of cell migration, RhoA activity was directly measured by G-LISA. RhoA activity was down-regulated by hCLEC-2 from 1 to 30 minutes after treatment (Figure 5E), suggesting that the regulatory effect of platelets on keratinocyte motility was partly mediated by down-regulating RhoA activity and by losing E-cadherin expression via the podoplanin/CLEC-2 signaling pathway.

The effects of major platelet releasates, such as bone morphogenetic protein-9, PF4, angiostatin, or endostatin, on keratinocyte migration were also examined. However, none of these platelet releasates modulated the migration of NHEKs or podoplanin mRNA levels (data not shown).

Overall, these results indicated that platelets down-regulated the function of podoplanin, leading to impaired motility of NHEKs in a CLEC-2–dependent manner.

Discussion

In this study, the possible functional mechanisms of podoplanin on keratinocytes in wounds were demonstrated. We observed that the expression of podoplanin began to increase shortly after wounding, and reached its peak after several days when bleeding had stopped and the platelet-rich clot was replaced by granulation tissue. Podoplanin up-regulation at the wound edge is thought to be mediated by STAT3b signaling.[10] Down-regulating podoplanin decreased the motility of keratinocytes, which is essential for re-epithelialization during wound healing. Wound healing is a dynamic, interactive process involving soluble mediators,

blood cells, extracellular matrix, and parenchymal cells.[25] Wound healing has three phases—inflammation, tissue formation, and tissue remodeling—that overlap in time. Commonly, re-epithelialization is seen from the middle of the tissue formation phase to the end of the tissue remodeling phase, but is not seen in the inflammation phase. Our findings that podoplanin was up-regulated at the time of re-epithelialization and that its disruption altered keratinocyte behavior suggested that podoplanin plays a pivotal role in re-epithelialization.

E-cadherin is a transmembrane glycoprotein and a mediator of calcium-dependent cell-cell adhesion in normal cells.[26] Several studies have reported that reduced expression of E-cadherin correlates with the expression of podoplanin and a poor prognosis in squamous cell carcinoma.[9,27,28] This suggests that the presence of podoplanin in oral squamous cell carcinoma cells is related to a migratory/invasive phenotype.[9] Thus, podoplanin might mediate cell motility via down-regulation of E-cadherin that contributes to the loss of cell adhesion in squamous carcinoma cells. Our study is, perhaps, the first to report that this migratory function of podoplanin is not restricted to tumor cells and is also found in normal keratinocytes during wound healing.

Platelets have multiple roles in wound healing.[25] During the initial step, tissue injury causes the disruption of blood vessels and extravasation of blood constituents. The blood clot re-establishes hemostasis and provides a provisional extracellular matrix for cell migration. Platelets not only facilitate the formation of a hemostatic plug but also secrete several mediators of wound healing, such as platelet-derived growth factor, that attract and activate macrophages and fibroblasts, which promote granulation tissue formation.[25] However, the effects of platelets on keratinocytes are not well understood. A single study reported that platelet lysates stimulated the migration and proliferation of keratinocytes.[15] However, the keratinocytes used therein were immortalized HaCaT cells, in which podoplanin is not expressed at basal levels.[15] Although we did not evaluate the podoplanin expression in HaCaT cells under platelet lysate exposure, we suggest that the stimulatory effects of platelets in that study might have been mediated instead by several growth factors released by platelets. On the basis of these findings, we evaluated whether platelets were involved in the migratory function of keratinocytes in wound healing, because platelets contain the CLEC-2 receptor. Our results indicate that platelets down-regulated podoplanin function, which led to a reduction in keratinocyte motility.

According to previous reports[25,29] and our present findings, we speculate that one of the important functions of platelets on wound healing is to delay re-epithelialization until wound bed preparation is completed (Figure 6). During the inflammatory phase, the wound bed is concave. Re-epithelialization within the depressed wound bed results in a severe scar. To prevent this, the platelet-rich aggregates promote the formation of granulation tissue that inhibits re-epithelialization on the surface of immature granulation tissue. During the tissue-remodeling phase, after platelet aggregates are replaced by granulation tissue and bleeding has stopped, the expression of podoplanin is up-regulated and re-epithelialization proceeds.

Finally, we evaluated whether the inhibitory effects of platelets on the motility of keratinocytes was because of direct signaling via CLEC-2 on podoplanin. In accordance with this supposition, we found that the administration of CLEC-2 decreased the motility of keratinocytes. Our results suggest that the concomitant up-regulation of E-cadherin expression and down-regulation of RhoA activity might be possible mechanisms of this inhibitory effect. In addition, a previous report indicated that the podoplanin/CLEC-2 interaction inhibited functions of lymphatic endothelial cells, such as proliferation, migration, and tube formation.[30] Of these, migration was thought to be inhibited partly through a contact-dependent mechanism because recombinant CLEC-2 inhibited the migration of lymphatic endothelial cells. However, most of these inhibitory effects were because of bone morphogenetic protein-9 released from platelets that became activated via the podoplanin/CLEC-2 interaction. In accordance with these observations, we investigated which platelet releasate was involved in the inhibitory effects of these cells on keratinocytes. Surprisingly, none of the platelet releasates tested, including bone morphogenetic protein-9, PF4, angiostatin, and endostatin, influenced the effects of podoplanin on keratinocytes, suggesting that the effects and mechanisms of podoplanin/CLEC-2 signaling in keratinocytes differed from those of platelet releasates.

In conclusion, the current study, although still speculative, provides data showing some possible mechanisms by which platelets might function as an inhibitory mediator on the motility of keratinocytes during wound healing. In addition, we demonstrated that podoplanin plays a pivotal role in re-epithelialization. Thus, the modulation of podoplanin might have therapeutic potential for treating impaired wound healing, such as occurs with diabetic foot ulcers.

Supplemental Data

Supplemental material for this article can be found at *http://dx.doi.org/10.1016/j.ajpath.2015.09.007.*

References

1. Rishi AK, Joyce-Brady M, Fisher J, Dobbs LG, Floros J, VanderSpek J, Brody JS, Williams MC: Cloning, characterization, and development expression of a rat lung alveolar type I cell gene in embryonic endodermal and neural derivatives. Dev Biol 1995, 167: 294–306
2. Breiteneder-Geleff S, Soleiman A, Horvat R, Amann G, Kowalski H, Kerjaschki D: [Podoplanin: a specific marker for lymphatic endothelium expressed in angiosarcoma]. German. Verh Dtsch Ges Pathol 1999, 83:270–275

3. Kan S, Konishi E, Arita T, Ikemoto C, Takenaka H, Yanagisawa A, Katoh N, Asai J: Podoplanin expression in cancer-associated fibroblasts predicts aggressive behavior in melanoma. J Cutan Pathol 2014, 41:561–567
4. Krishnan H, Ochoa-Alvarez JA, Shen Y, Nevel E, Lakshminarayanan M, Williams MC, Ramirez MI, Miller WT, Goldberg GS: Serines in the intracellular tail of podoplanin (PDPN) regulate cell motility. J Biol Chem 2013, 288:12215–12221
5. Ochoa-Alvarez JA, Krishnan H, Shen Y, Acharya NK, Han M, McNulty DE, Hasegawa H, Hyodo T, Senga T, Geng JG, Kosciuk M, Shin SS, Goydos JS, Temiakov D, Nagele RG, Goldberg GS: Plant lectin can target receptors containing sialic acid, exemplified by podoplanin, to inhibit transformed cell growth and migration. PLoS One 2012, 7:e41845
6. Shen Y, Chen CS, Ichikawa H, Goldberg GS: SRC induces podoplanin expression to promote cell migration. J Biol Chem 2010, 285: 9649–9656
7. Kato Y, Kaneko M, Sata M, Fujita N, Tsuruo T, Osawa M: Enhanced expression of Aggrus (T1alpha/podoplanin), a platelet-aggregation-inducing factor in lung squamous cell carcinoma. Tumour Biol 2005, 26:195–200
8. Schacht V, Dadras SS, Johnson LA, Jackson DG, Hong YK, Detmar M: Up-regulation of the lymphatic marker podoplanin, a mucin-type transmembrane glycoprotein, in human squamous cell carcinomas and germ cell tumors. Am J Pathol 2005, 166:913–921
9. Martin-Villar E, Scholl FG, Gamallo C, Yurrita MM, Munoz-Guerra M, Cruces J, Quintanilla M: Characterization of human PA2.26 antigen (T1alpha-2, podoplanin), a small membrane mucin induced in oral squamous cell carcinomas. Int J Cancer 2005, 113:899–910
10. Honma M, Minami-Hori M, Takahashi H, Iizuka H: Podoplanin expression in wound and hyperproliferative psoriatic epidermis: regulation by TGF-beta and STAT-3 activating cytokines, IFN-gamma, IL-6, and IL-22. J Dermatol Sci 2012, 65:134–140
11. Honma M, Fujii M, Iinuma S, Minami-Hori M, Takahashi H, Ishida-Yamamoto A, Iizuka H: Podoplanin expression is inversely correlated with granular layer/filaggrin formation in psoriatic epidermis. J Dermatol 2013, 40:296–297
12. Suzuki-Inoue K, Fuller GL, Garcia A, Eble JA, Pohlmann S, Inoue O, Gartner TK, Hughan SC, Pearce AC, Laing GD, Theakston RD, Schweighoffer E, Zitzmann N, Morita T, Tybulewicz VL, Ozaki Y, Watson SP: A novel Syk-dependent mechanism of platelet activation by the C-type lectin receptor CLEC-2. Blood 2006, 107:542–549
13. Suzuki-Inoue K, Kato Y, Inoue O, Kaneko MK, Mishima K, Yatomi Y, Yamazaki Y, Narimatsu H, Ozaki Y: Involvement of the snake toxin receptor CLEC-2, in podoplanin-mediated platelet activation, by cancer cells. J Biol Chem 2007, 282:25993–26001
14. Kato Y, Kaneko MK, Kunita A, Ito H, Kameyama A, Ogasawara S, Matsuura N, Hasegawa Y, Suzuki-Inoue K, Inoue O, Ozaki Y, Narimatsu H: Molecular analysis of the pathophysiological binding of the platelet aggregation-inducing factor podoplanin to the C-type lectin-like receptor CLEC-2. Cancer Sci 2008, 99:54–61
15. Ranzato E, Patrone M, Mazzucco L, Burlando B: Platelet lysate stimulates wound repair of HaCaT keratinocytes. Br J Dermatol 2008, 159:537–545
16. Martin-Villar E, Megias D, Castel S, Yurrita MM, Vilaro S, Quintanilla M: Podoplanin binds ERM proteins to activate RhoA and promote epithelial-mesenchymal transition. J Cell Sci 2006, 119: 4541–4553
17. Greenhalgh DG, Sprugel KH, Murray MJ, Ross R: PDGF and FGF stimulate wound healing in the genetically diabetic mouse. Am J Pathol 1990, 136:1235–1246
18. Asai J, Takenaka H, Hirakawa S, Sakabe J, Hagura A, Kishimoto S, Maruyama K, Kajiya K, Kinoshita S, Tokura Y, Katoh N: Topical simvastatin accelerates wound healing in diabetes by enhancing angiogenesis and lymphangiogenesis. Am J Pathol 2012, 181: 2217–2224
19. Asai J, Takenaka H, Katoh N, Kishimoto S: Dibutyryl cAMP influences endothelial progenitor cell recruitment during wound neovascularization. J Invest Dermatol 2006, 126:1159–1167
20. Asai J, Takenaka H, Kusano KF, Li M, Luedemann C, Curry C, Eaton E, Iwakura A, Tsutsumi Y, Hamada H, Kishimoto S, Thorne T, Kishore R, Losordo DW: Topical sonic hedgehog gene therapy accelerates wound healing in diabetes by enhancing endothelial progenitor cell-mediated microvascular remodeling. Circulation 2006, 113:2413–2424
21. Committee for the Update of the Guide for the Care and Use of Laboratory Animals; National Research Council: Guide for the Care and Use of Laboratory Animals: Eighth Edition. Washington, DC, National Academies Press, 2011
22. Suzuki-Inoue K, Inoue O, Frampton J, Watson SP: Murine GPVI stimulates weak integrin activation in PLCgamma2-/- platelets: involvement of PLCgamma1 and PI3-kinase. Blood 2003, 102:1367–1373
23. Abràmoff MD, Magalhães PJ, Ram SJ: Image processing with ImageJ. Biophoto Int 2004, 11:36–42
24. Cavallaro U, Schaffhauser B, Christofori G: Cadherins and the tumour progression: is it all in a switch? Cancer Lett 2002, 176:123–128
25. Singer AJ, Clark RA: Cutaneous wound healing. N Engl J Med 1999, 341:738–746
26. Wijnhoven BP, Dinjens WN, Pignatelli M: E-cadherin-catenin cell-cell adhesion complex and human cancer. Br J Surg 2000, 87:992–1005
27. Nakashima Y, Yoshinaga K, Kitao H, Ando K, Kimura Y, Saeki H, Oki E, Morita M, Kakeji Y, Hirahashi M, Oda Y, Maehara Y: Podoplanin is expressed at the invasive front of esophageal squamous cell carcinomas and is involved in collective cell invasion. Cancer Sci 2013, 104:1718–1725
28. Toll A, Masferrer E, Hernandez-Ruiz ME, Ferrandiz-Pulido C, Yebenes M, Jaka A, Tuneu A, Juegla A, Gimeno J, Baro T, Casado B, Gandarillas A, Costa I, Mojal S, Pena R, de Herreros AG, Garcia-Patos V, Pujol RM, Hernandez-Munoz I: Epithelial to mesenchymal transition markers are associated with an increased metastatic risk in primary cutaneous squamous cell carcinomas but are attenuated in lymph node metastases. J Dermatol Sci 2013, 72: 93–102
29. Galliera E, Corsi MM, Banfi G: Platelet rich plasma therapy: inflammatory molecules involved in tissue healing. J Biol Regul Homeost Agents 2012, 26:35S–42S
30. Osada M, Inoue O, Ding G, Shirai T, Ichise H, Hirayama K, Takano K, Yatomi Y, Hirashima M, Fujii H, Suzuki-Inoue K, Ozaki Y: Platelet activation receptor CLEC-2 regulates blood/lymphatic vessel separation by inhibiting proliferation, migration, and tube formation of lymphatic endothelial cells. J Biol Chem 2012, 287: 22241–22252

Inhibition of IgE-mediated allergic reactions by pharmacologically targeting the circadian clock

Yuki Nakamura, PhD,[a] Nobuhiro Nakano, PhD,[b] Kayoko Ishimaru,[a] Noriko Ando, MD,[c] Ryohei Katoh, MD, PhD,[d] Katsue Suzuki-Inoue, MD, PhD,[e] Satoru Koyanagki, PhD,[f] Hideoki Ogawa, MD, PhD,[b] Ko Okumura, MD, PhD,[b] Shigenobu Shibata, PhD,[g] and Atsuhito Nakao, MD, PhD[a,b] *Yamanashi, Tokyo, and Fukuoka, Japan*

Background: The circadian clock temporally gates signaling through the high-affinity IgE receptor (FcεRI) in mast cells, thereby generating a marked day/night variation in allergic reactions. Thus manipulation of the molecular clock in mast cells might have therapeutic potential for IgE-mediated allergic reactions.

Objective: We determined whether pharmacologically resetting the molecular clock in mast cells or basophils to times when FcεRI signaling was reduced (ie, when core circadian protein period 2 [PER2] is upregulated) resulted in suppression of IgE-mediated allergic reactions.

Methods: We examined the effects of PF670462, a selective inhibitor of the key clock component casein kinase 1δ/ε, or glucocorticoid, both of which upregulated PER2 in mast cells, on IgE-mediated allergic reactions both *in vitro* and *in vivo*.

Results: PF670462 or corticosterone (or dexamethasone) suppressed IgE-mediated allergic reactions in mouse bone marrow–derived mast cells or basophils and passive cutaneous anaphylactic reactions in mice in association with increased PER2 levels in mast cells or basophils. PF670462 or dexamethasone also ameliorated allergic symptoms in a mouse model of allergic rhinitis and downregulated allergen-specific basophil reactivity in patients with allergic rhinitis.

Conclusion: Pharmacologically resetting the molecular clock in mast cells or basophils to times when FcεRI signaling is reduced can inhibit IgE-mediated allergic reactions. The results suggest a new strategy for controlling IgE-mediated allergic diseases. Additionally, this study suggests a novel mechanism underlying the antiallergic actions of glucocorticoids that relies on the circadian clock, which might provide a novel insight into the pharmacology of this drug in allergic patients. (J Allergy Clin Immunol 2015;■■■:■■■-■■■.)

Key words: *Circadian clock, mast cells, basophils, IgE, allergy*

The circadian clock plays a crucial role in the temporal regulation of behavior and physiology, including immunity.[1-7] In mammals the light-entrained central oscillator located in the suprachiasmatic nucleus (SCN) of the hypothalamus synchronizes peripheral oscillators present in nearly all cell types, including mast cells, through neural and endocrine pathways.[1,2] The molecular mechanisms of rhythm generation are highly conserved in the SCN and peripheral cells and created and maintained by interlocked transcriptional-translational feedback loops with a 24-hour period.[1-3] The core feedback loop is driven by 4 clock proteins, 2 activators (circadian locomotor output cycles kaput [CLOCK] and brain and muscle Arnt-like 1 [BMAL1]) and 2 repressors (period [PER] and cryptochrome [CRY]), as well as kinases and phosphatases that regulate the localization and stability of these clock proteins (eg, casein kinase [CK] 1δ/ε). Briefly, CLOCK and BMAL1 heterodimerize and activate transcription of the *Per1* and *Per2* and *Cry1* and *Cry2* genes, as well as other clock-controlled output genes, through E-box or E-box–like elements in the promoter regions of those genes. The PER1/2 and CRY1/2 proteins, in turn, inhibit their own expression by repressing CLOCK/BMAL1 activity. CK1δ and CK1ε play a critical role in the posttranslational modification of the circadian timing system.[8] CK1δ and CK1ε phosphorylate the PER proteins, leading to their ubiquitin-dependent degradation and determine the intrinsic period of the clock. Therefore inhibition of CK1δ/ε slows down PER protein turnover, decelerates clock progression, and lengthens the circadian period.[8]

Recently, the circadian clock has been shown to drive a time of day–dependent variation in IgE/mast cell–mediated allergic reactions in mice.[9-11] The mast cell–intrinsic clock temporally gates FcεRI signaling in mast cells: specifically, FcεRI signaling is reduced at times when the core clock protein PER2 is highly expressed in mast cells (ie, during the active phase in mice).[11] PER2 likely does so in mast cells by inhibiting CLOCK/BMAL1 activity, which regulates expression of the β subunit of FcεRI (FcεRIβ), an amplifier of FcβRI expression and signaling,[12] in a circadian manner through binding to the E-box–like elements in the promoter region of *FCERIB*.[11]

Therefore we hypothesized that pharmacologically resetting the molecular clock in mast cells to times when FcεRI signaling is reduced (ie, when PER2 is upregulated) might inhibit IgE-mediated allergic reactions. To test the hypothesis, this study examined the effects of PF670462, a well-established selective inhibitor of CK1δ/ε, which prevented the degradation of PER2 and upregulated PER2 levels,[8,13-15] or corticosterone, which upregulated *Per2* mRNA and protein levels in mast cells,[11] on IgE-mediated allergic reactions both *in vitro* and *in vivo*.

From the Departments of [a]Immunology, [c]Dermatology, [d]Pathology, and [e]Clinical and Laboratory Medicine, University of Yamanashi Faculty of Medicine; [b]the Atopy Research Center, Juntendo University School of Medicine, Tokyo; [f]the Department of Pharmaceutics, Graduate School of Pharmaceutical Sciences, Fukuoka; and [g]the Department of Physiology and Pharmacology, School of Advanced Science and Engineering, Waseda University, Tokyo.

Supported in part by JSPS KAKEN grant no. 90580465 from the Ministry of Education, Culture, Sports, Science, and Technology, Japan.

Disclosure of potential conflict of interest: A. Nakao has received research support from Japan's Ministry of Education, Culture, Sports, Science, and Technology. The rest of the authors declare that they have no relevant conflicts of interest.

Received for publication November 2, 2014; revised July 26, 2015; accepted for publication August 18, 2015.

Corresponding author: Atsuhito Nakao, MD, PhD, Department of Immunology, Faculty of Medicine, University of Yamanashi, 1110 Shimokato, Chuo, Yamanashi 409-3898, Japan. E-mail: anakao@yamanashi.ac.jp.

0091-6749/$36.00

http://dx.doi.org/10.1016/j.jaci.2015.08.052

Abbreviations used
BMAL1: Brain and muscle Arnt-like 1
BMMC: Bone marrow–derived mast cell
cAMP: Cyclic AMP
CK: Casein kinase
CLOCK: Circadian locomotor output cycles kaput
CRY: Cryptochrome
DEX: Dexamethasone
JCP: Japanese cedar pollen
OVA: Ovalbumin
PCA: Passive cutaneous anaphylaxis
PER: Period
SCN: Suprachiasmatic nucleus
ZT: Zeitgeber time

METHODS

For more information, see the Methods section in this article's Online Repository at www.jacionline.org.

RESULTS

PF670462 or corticosterone suppresses IgE-mediated allergic reactions associated with increased PER2 levels in mast cells *in vitro*

We examined the effects of PF670462 or corticosterone on mast cell clockwork (PER2 levels) and IgE-mediated mast cell reactions *in vitro*. Based on monitoring of bioluminescent emission of bone marrow–derived mast cells (BMMCs) from *Per2*^{Luc} knock-in mice, which express PER2 as a luciferase fusion protein (PER2^{LUC} BMMCs),[16] under *in vitro* culture conditions, the time window during which the mast cell clockwork was functional was limited (0-48 hours after a media change for synchronization; Fig 1, *A*).[9,11] Addition of PF670462 (10 μmol/L; a dose that can inhibit both CK1δ and CK1ε activity)[15] or corticosterone (300 nmol/L) 72 hours after the media change (ie, under unsynchronized conditions) significantly increased PER2^{LUC} levels 4 hours later (Fig 1, *A*).

At that time point, PER2^{LUC} BMMCs were sensitized with IgE and stimulated with anti-IgE antibody. IgE-mediated degranulation was inhibited in both PF670462- or corticosterone-treated PER2^{LUC} BMMCs in association with suppression of FcεRI signaling (intracellular Ca^{2+} mobilization and total tyrosine phosphorylation of intracellular proteins; Fig 1, *B-D*). When PER2^{LUC} BMMCs were treated with PF670462 or corticosterone for 15 minutes 72 hours after the media change and then sensitized with IgE, followed by stimulation with anti-IgE antibody, these inhibitory effects were not observed, possibly excluding clock-unrelated or other nonspecific effects (Fig 1, *B-D*). Similar findings were observed in BMMCs from wild-type mice (see Fig E1 in this article's Online Repository at www.jacionline.org). Importantly, the suppressive effects were not observed in PER2^{LUC} BMMCs with a loss-of-function mutation in the key circadian gene *Clock* (*Clock*$^{\Delta 19/\Delta 19}$ PER2^{LUC} BMMCs),[17] in which PF670462 or corticosterone marginally increased PER2 levels (Fig 1, *A-D*). Neither PF670462 nor corticosterone affected cellular viability or baseline cellular bioenergetics of PER2^{LUC} BMMCs (see Figs E2 and E3 in this article's Online Repository at www.jacionline.org). Wild-type BMMCs indeed expressed CK1δ protein (see Fig E4 in this article's Online Repository at www.jacionline.org). Thus resetting (or resynchronizing) the mast cell clock with PF670462 or corticosterone suppressed IgE-mediated reactions associated with increased PER2 levels in mast cells.

We also found that another CK1δ/ε inhibitor, D4476,[18] suppressed IgE-mediated degranulation in wild-type BMMCs associated with increased PER2 levels (see Fig E5 in this article's Online Repository at www.jacionline.org). Furthermore, neither PF670462 nor corticosterone suppressed IgE-mediated degranulation in BMMCs derived from mice with a loss-of-function mutation of *Per2* (*mPer2*$^{m/m}$ mice; see Fig E6, *A*, in this article's Online Repository at www.jacionline.org).[19]

Additionally, we found that a selective inhibitor of CK1ε, PF4800567, which confers greater than 20-fold selective inhibition over CK1δ,[13,20] did not increase PER2 levels and did not affect IgE-mediated degranulation in PER2^{LUC} BMMCs, suggesting that inhibition of CK1δ by PF670462 was more important for this suppressive activity than inhibition of CK1ε (see Fig E7 in this article's Online Repository at www.jacionline.org).

PF670462 or corticosterone suppresses IgE-mediated allergic reactions in IgE-sensitized mast cells, as well as unsensitized mast cells, *in vitro*

We further examined the effects of PF670462 or corticosterone on mast cells that were already sensitized with IgE. The time window during which the mast cell clockwork was functional was not affected regardless of whether mast cells were sensitized or unsensitized with IgE (0-48 hours after a media change for synchronization; see Fig E8, *A*, in this article's Online Repository at www.jacionline.org). Addition of PF670462 or corticosterone, but not PF4800567, 72 hours after the media change (ie, under unsynchronized conditions) significantly increased PER2^{LUC} levels 4 hours later in IgE-sensitized PER2^{LUC} BMMCs, as well as in unsensitized PER2^{LUC} BMMCs (see Fig E8, *A*).

At that time point, the PER2^{LUC} BMMCs were stimulated with anti-IgE antibody. IgE-mediated degranulation was inhibited in both PF670462- or corticosterone-treated, but not PF4800567-treated, IgE-sensitized PER2^{LUC} BMMCs (see Fig E8, *B*). Thus PF670462 or corticosterone suppressed IgE-mediated degranulation in mast cells in association with increased PER2 levels, regardless of whether mast cells were sensitized or unsensitized with IgE.

PF670462 or corticosterone suppresses FcεRI expression in mast cells

To investigate how PF670462 or corticosterone inhibited IgE-mediated degranulation in mast cells, we examined the effects of P670462 or corticosterone on cell-surface FcεRI expression on mast cells. Addition of PF670462 (10 μmol/L) or corticosterone (300 nmol/L) 72 hours after the media change (ie, under unsynchronized conditions) significantly suppressed FcεRI expression in wild-type, but not *Clock*-mutated or *Per2*-mutated, BMMCs 4 hours but not 15 minutes after the treatments (Fig 1, *E*, and see Fig E6, *B*). D4476 also suppressed FcεRI expression in wild-type BMMCs 4 hours but not 15 minutes after the treatment (see Fig E5, *C*). The inhibitory effects of PF670462 or corticosterone on FcεRI expression were also observed when IgE-sensitized BMMCs were treated with PF670462 or corticosterone, but not PF4800567, for 4 hours (see Fig E8, *C*). Furthermore, peritoneal mast cells isolated from wild-type mice 4 hours

after the treatment with PF670462 (50 mg/kg per mouse) exhibited reduced FcεRI expression (Fig 1, *F*). Thus these reagents likely suppressed IgE-mediated reactions in mast cells by downregulating FcεRI levels.

Importantly, wild-type BMMCs overexpressing PER2 by retroviral vectors exhibited reduced cell-surface FcεRI expression, IgE-mediated intracellular Ca^{2+} mobilization, and degranulation when compared with control BMMCs (see Fig E9, *A-D*, in this article's Online Repository at www.jacionline.org). Conversely, BMMCs from *Per2*-muated mice ($mPer2^{m/m}$ mice) exhibited increases in cell-surface FcεRI expression and IgE-mediated degranulation when compared with wild-type BMMCs (see Fig E9, *E* and *F*). Collectively, it is plausible that PF670462- or corticosterone-induced PER2 is critical for suppression of FcεRI expression and signaling in mast cells.

Aminophylline suppresses IgE-mediated allergic reactions associated with increased PER2 levels in mast cells *in vitro*

The circadian clock is reset by environmental time cues, such as light, to synchronize with the external 24-hour cycles. The molecular mechanisms of entrainment are not fully understood, but the cyclic AMP (cAMP)/cAMP response element-binding protein pathway induced by light or hormones is considered to be important for signaling to entrain the SCN and peripheral clocks by regulating expression of "clock genes."[1-3] Activation of cAMP signaling increases transcription of *Per2* through the cAMP-responsive element in the promoter region of *Per2* and regulates PER2 protein levels.[21]

To further test the hypothesis that pharmacologically resetting the molecular clock in mast cells to times when FcεRI signaling is reduced (ie, when PER2 is upregulated) might inhibit IgE-mediated allergic reactions, we examined the effects of aminophylline, an inhibitor of phosphodiesterases that activates cAMP signaling,[22] on the circadian clock and FcεRI expression/signaling in mast cells.

Similar to PF670462 or corticosterone, aminophylline increased PER2 levels and inhibited FcεRI expression and IgE-mediated degranulation in wild-type, but not *Clock*-mutated, BMMCs 4 hours after the treatment (see Fig E10 in this article's Online Repository at www.jacionline.org). These results suggest that aminophylline suppresses IgE-mediated allergic reactions associated with increased PER2 levels in mast cells, also supporting the antiallergic function of PER2 in mast cells.

PF670462 or dexamethasone suppresses IgE-mediated allergic reactions associated with increased PER2 levels in mast cells *in vivo*

We further examined the effects of PF670462 and the synthetic steroid dexamethasone (DEX) on the passive cutaneous anaphylactic (PCA) reaction[9,11] and in an allergic rhinitis model.[23]

In vivo imaging with mast cell–deficient mice subcutaneously reconstituted with $PER2^{LUC}$ BMMCs revealed that $PER2^{LUC}$ bioluminescence exhibited a time of day–dependent variation, with a maximum at 10 PM (Zeitgeber time [ZT] 16; the light in the mouse facility was turned on at 6 AM [ZT 0]) and a minimum at 10 AM (ZT4; see Fig E11 in this article's Online Repository at www.jacionline.org), as previously described.[9,11] Treatment of the mice with PF670462 or DEX at ZT4 (the nadir of $PER2^{LUC}$ levels in mast cells) increased $PER2^{LUC}$ levels 4 hours later at ZT8 (Fig 2, *A* and *B* and Fig 3, *A* and *B*), suggesting that these reagents increased PER2 levels in mast cells *in vivo*.

The extent of the PCA reaction at ZT8 in the mice pretreated with PF670462 or DEX at ZT4 was suppressed relative to that seen in mice pretreated with vehicle at ZT4 associated with serum monocyte chemoattractant protein 1 levels (Fig 2, *C-E*, and Fig 3, *C-E*). Serum corticosterone and IgE levels at ZT8 were comparable between vehicle- and PF670462-treated mice (Fig 2, *F*). By contrast, similar findings were not observed in mast cell–deficient mice reconstituted with $Clock^{\Delta 19/\Delta 19}$ $PER2^{LUC}$ BMMCs (Fig 2, *A-E*; Fig 3, *A-E*; and see Fig E11). The numbers of mast cells in the skin became comparable between the mice reconstituted with wild-type BMMCs and those reconstituted with *Clock*-mutated BMMCs in the current experimental design (see Fig E12 in this article's Online Repository at www.jacionline.org). Thus resetting (phase-shifting) the mast cell clock by using PF670462 or DEX suppressed the PCA reaction associated with increased PER2 levels in mast cells.

Continuous intranasal challenge with ovalbumin (OVA) in OVA-sensitized mice induces phenotypes that recapitulate allergic rhinitis, which is IgE and mast cell dependent.[23] Similar to the findings in PCA reactions, intranasal administration of PF670462 or DEX at ZT4, followed by nasal challenge with OVA at ZT8, in OVA-sensitized mice suppressed the frequency of OVA-induced nose scratching and sneezing when compared with that in vehicle-treated OVA-sensitized mice (Fig 4, *A*). Serum OVA-specific IgE levels were comparable between vehicle-, PF670462-, and DEX-treated OVA-sensitized mice (Fig 4, *B*). We confirmed that OVA-induced nose scratching and sneezing in OVA-sensitized mice was largely mast cell dependent because the frequency of these symptoms significantly increased in mast cell–deficient W/Wv mice reconstituted with wild-type BMMCs when compared with the frequency observed in W/Wv mice (see Fig E13 in this article's Online Repository at www.jacionline.org). These findings suggest that pretreatment with PF670462 or DEX 4 hours before the final OVA challenge can suppress OVA-mediated allergic symptoms in a mouse model of allergic rhinitis.

PF670462 or corticosterone suppresses IgE-mediated allergic reactions in mouse and human basophils

Finally, we investigated whether PF670462 or corticosterone could affect IgE-mediated allergic reactions in basophils, as well as in mast cells. Most recently, we reported that, similar to BMMCs, the bone marrow–derived basophils derived from $Per2^{Luc}$ knock-in mice ($PER2^{LUC}$ BM basophils) showed circadian expression of $PER2^{LUC}$ protein 0 to 48 hours after a media change for synchronization.[24] Furthermore, IgE-mediated histamine and IL-4 releases in $PER2^{LUC}$ bone marrow–derived basophils exhibited a time of day–dependent variation relying on the normal activity of *Clock* in basophils.[24] Therefore basophils, as well as mast cells, have functional clockwork, which temporally gates IgE-mediated allergic reactions in basophils.

Addition of PF670462 (10 μmol/L) or corticosterone (300 nmol/L) 72 hours after the media change (ie, under unsynchronized conditions) significantly increased $PER2^{LUC}$ levels 4 hours later in wild-type, but not *Clock*-mutated, $PER2^{LUC}$ bone marrow–derived basophils (Fig 5, *A*). At that time point, $PER2^{LUC}$ bone marrow–derived basophils were sensitized with IgE and

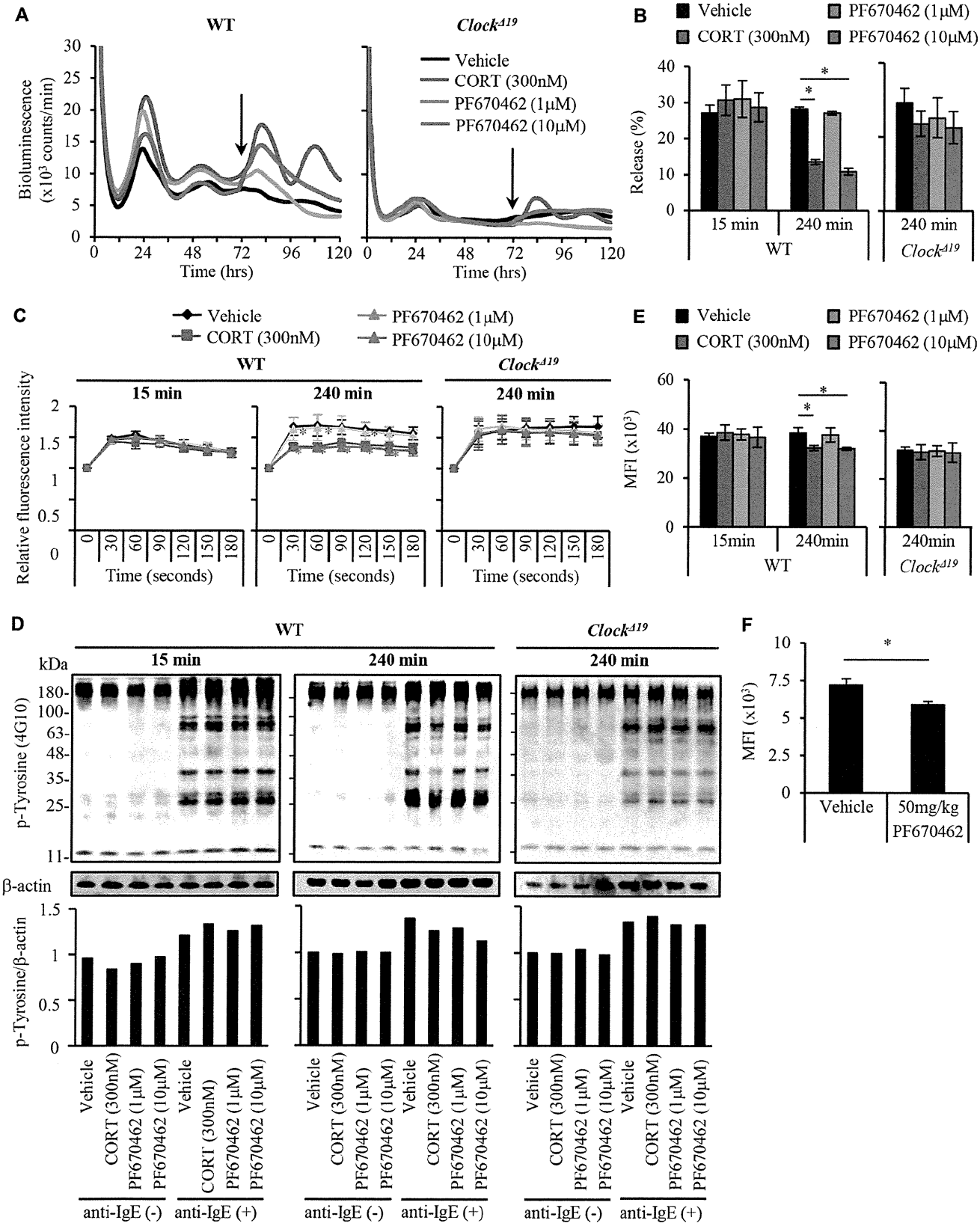

FIG 1. PF670462 or corticosterone suppresses IgE-mediated allergic reactions in wild-type *(WT)*, but not *Clock*-mutated, mast cells associated with increased PER2 levels. **A**, PER2^{LUC} bioluminescence of BMMCs derived from *Per2*^{Luc} knock-in mice (PER2^{LUC} BMMCs) with or without *Clock* mutation (WT or *Clock*^{Δ19}).

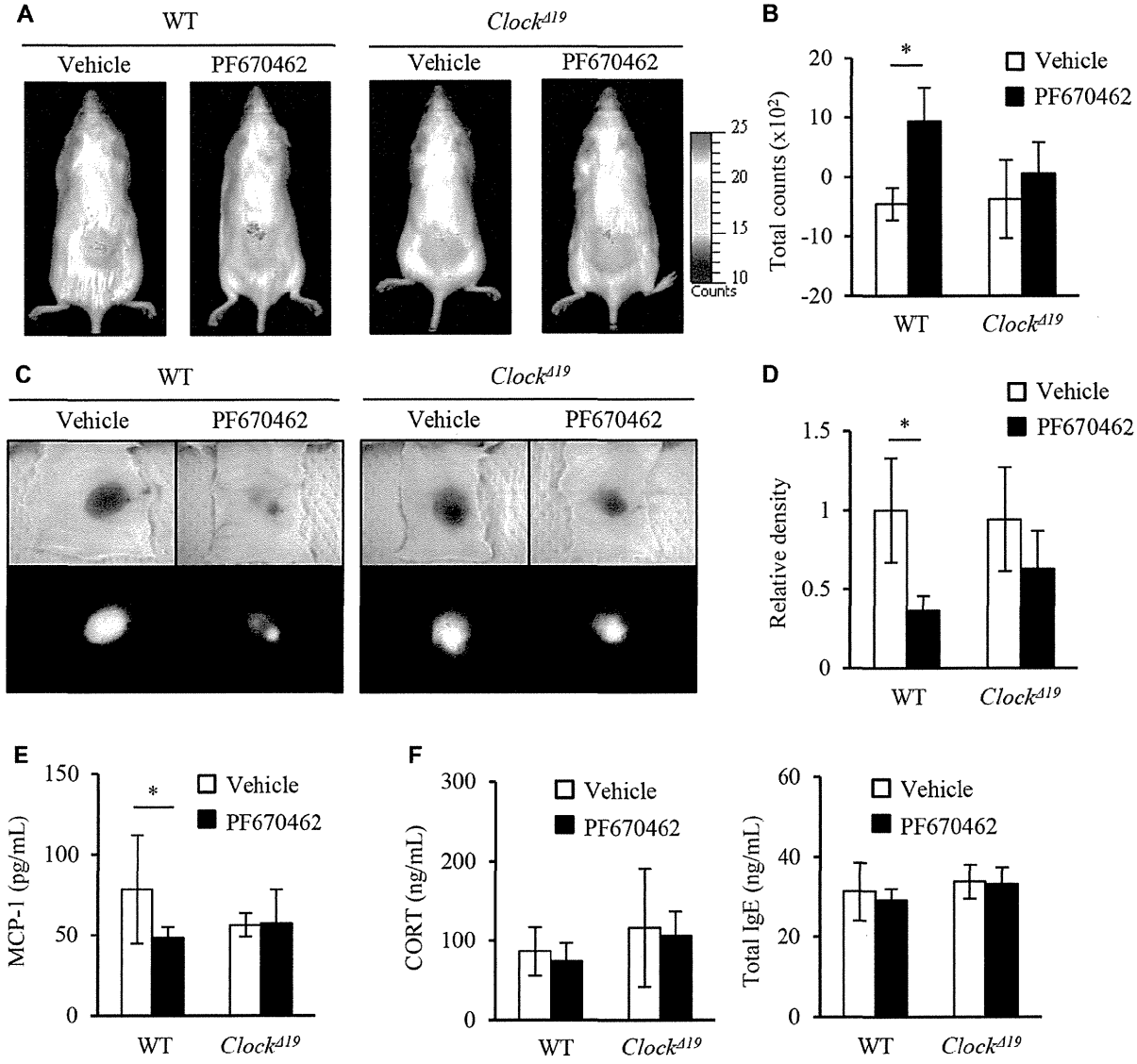

FIG 2. PF670462 suppresses PCA reactions associated with increased PER2 levels in mast cells. **A,** Representative pictures of *in vivo* imaging of mast cell–deficient mice reconstituted with subcutaneous injections of BMMCs derived from *Per2*^{Luc} knock-in mice with or without *Clock* mutation (PER2^{LUC} BMMCs or *Clock*$^{\Delta 19}$ PER2^{LUC} BMMCs). Mice were treated with PF670462 (50 mg/kg administered intraperitoneally) or vehicle at ZT4 (10 AM), and the pictures were taken at ZT8 (2 PM). **B,** Quantitative analysis of the data in Fig 2, *A* (n = 5). **C,** Representative pictures of the skin color reactions at ZT8 in mast cell–deficient mice reconstituted with subcutaneous injections of PER2^{LUC} BMMCs or *Clock*$^{\Delta 19}$ PER2^{LUC} BMMCs *(upper panels)* and digitized images used for density value evaluations *(lower panels)*. Reconstituted mice were treated with PF670462 (50 mg/kg administered intraperitoneally) or vehicle at ZT4, and PCA reactions were induced at ZT8. **D,** Quantitative analysis of the data in Fig 2, *C* (n = 5). **E,** Serum monocyte chemoattractant protein 1 (*MCP-1*; CCL2) levels 30 minutes after induction of PCA reactions, as described in Fig 2, *C* (n = 5). **F,** Serum corticosterone and total IgE levels at ZT8, as described in Fig 2, *C* (n = 5). Values represent means ± SDs. *$P < .05$.

PF670462 or corticosterone was added at 72 hours after the media change, as indicated by the *arrows*. **B,** IgE-mediated release of β-hexosaminidase in wild-type and *Clock*-mutated PER2^{LUC} BMMCs (n = 6). **C,** IgE-dependent intracellular Ca^{2+} mobilization in wild-type and *Clock*-mutated PER2^{LUC} BMMCs (n = 4). **D,** IgE-dependent total tyrosine phosphorylation levels in wild-type and *Clock*-mutated PER2^{LUC} BMMCs. *Upper panels,* Representative pictures; *lower panels,* quantitative analysis. **E,** FcεRIα levels on wild-type and *Clock*-mutated PER2^{LUC} BMMCs (n = 4). **F,** FcεRIα levels on peritoneal mast cells (n = 10). *CORT,* Corticosterone; *MFI,* mean fluorescence intensity. Values represent means ± SDs. *$P < .05$.

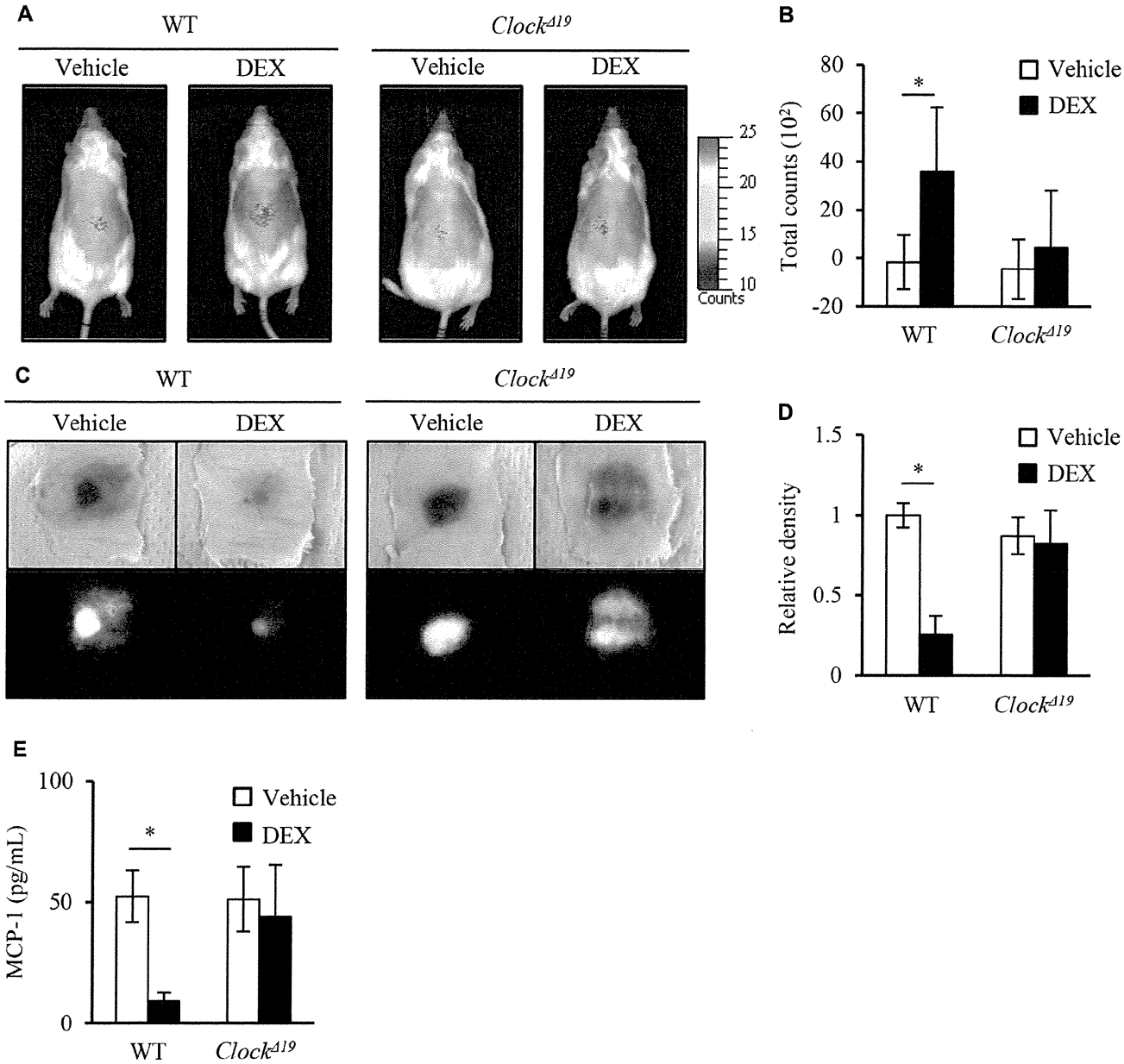

FIG 3. DEX suppresses the PCA reaction associated with increased PER2 levels in mast cells. **A,** Representative pictures of *in vivo* imaging of mast cell–deficient mice reconstituted with subcutaneous injections of BMMCs derived from *Per2*^{Luc} knock-in mice with or without *Clock* mutation (PER2^{LUC} BMMCs or *Clock*$^{\Delta 19}$ PER2^{LUC} BMMCs). The mice were treated with DEX (50 mg/kg administered intraperitoneally) or vehicle at ZT4 (AM10:00), and the pictures were taken at ZT8 (PM 2:00). **B,** Quantitative analysis of the data in Fig 3, *A* (n = 3-4). **C,** Representative pictures of the skin color reactions at ZT8 in mast cell–deficient mice reconstituted with subcutaneous injections of PER2^{LUC} BMMCs or *Clock*$^{\Delta 19}$ PER2^{LUC} BMMCs *(upper panels)* and digitalized images for the density value evaluations *(lower panels)*. Reconstituted mice were treated with DEX (50 mg/kg administered intraperitoneally) or vehicle at ZT4, and PCA reactions were induced at ZT8. **D,** Quantitative analysis of the data in Fig 3, *C* (n = 3-4). **E,** Serum monocyte chemoattractant protein 1 (*MCP-1*; CCL2) levels 30 minutes after induction of PCA reactions, as described in Fig 3, *C* (n = 3-4). *WT,* Wild-type. Values represent means ± SDs. **P* < .05.

stimulated with anti-IgE antibody. Production of IgE-mediated histamine and IL-4 was inhibited in both PF670462- and corticosterone-treated, but not PF4800567-treated, PER2^{LUC} bone marrow–derived basophils (Fig 5, *B*). Furthermore, addition of PF670462 or corticosterone, but not PF4800567, 72 hours after the media change (ie, under unsynchronized conditions) significantly suppressed FcεRI expression in wild-type, but not *Clock*-mutated, PER2^{LUC} bone marrow–derived basophils 4 hours but not 15 minutes after the treatments (Fig 5, *C*).

Similar findings were also obtained in human basophils. Basophils isolated from peripheral blood of healthy nonatopic volunteers were pretreated with PF670462 or PF4800567 for 15

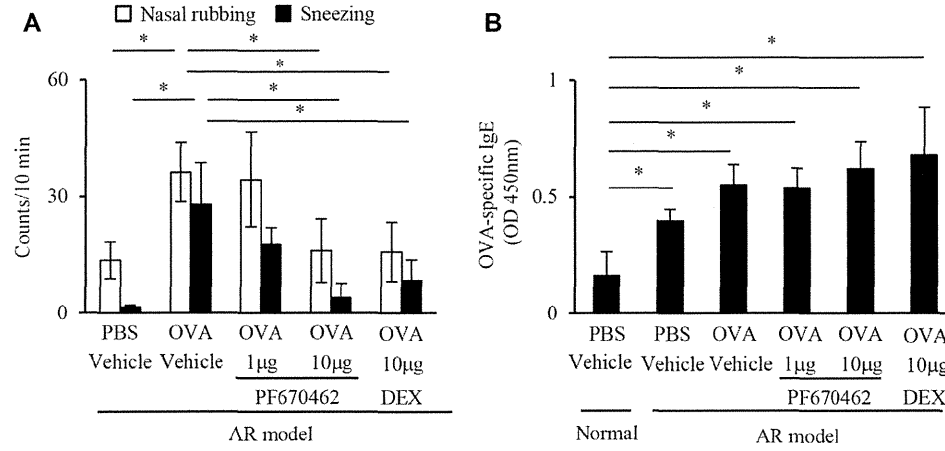

FIG 4. PF670462 suppresses IgE-mediated allergic symptoms in an allergic rhinitis *(AR)* model. **A,** The frequency of nasal rubbing or sneezing was counted for a 10-minute period after the last intranasal challenge with OVA (n = 5-6). **B,** OVA-specific IgE levels in the serum of unsensitized (normal) or sensitized (AR model) mice (n = 5-6). Values represent means ± SDs. *$P < .05$.

minutes or 4 hours and then stimulated with anti-IgE antibody. Treatment of human basophils with PF670462, but not PF4800567, for 4 hours but not 15 minutes inhibited IgE-mediated histamine and IL-4 production associated with suppression of FcεRI expression (Fig 5, *D* and *E*).

CD203c is an activation marker upregulated by cross-linking of FcεRI in human basophils.[25] Most recently, we reported that allergen-induced CD203c expression on basophils exhibited a time of day–dependent variation in patients with allergic rhinitis caused by Japanese cedar pollen (JCP) associated with temporal variations of canonical circadian clock gene expression.[24] To determine whether the inhibitory effects of PF670462 on IgE-mediated basophil responses were relevant to human allergic diseases, we examined the effects of PF670462 on allergen-induced CD203c expression on basophils isolated from patients with Japanese cedar pollinosis.

Pretreatment of basophils with PF670462, but not PF4800567, for 4 hours (but not 15 minutes) before JCP stimulation inhibited JCP-induced CD203c upregulation (Fig 5, *F*). Overall, these findings suggest that resetting (or resynchronizing) the basophil clock with PF670462 or corticosterone suppressed IgE/basophil-mediated allergic reactions associated with increased PER2 levels.

DISCUSSION

This study argues that PF670462 or corticosterone (or DEX) suppressed IgE/mast cell–mediated allergic reactions, relying on the intact mast cell clockwork because (1) PF670462 or corticosterone did not affect IgE-mediated allergic reactions in *Clock*-mutated or *Per2*-mutated mast cells, where these reagents failed to increase PER2 levels or PER2 did not function properly (Figs 1-3 and see Fig E6); (2) PF670462 or corticosterone did not affect IgE-mediated allergic reactions when these reagents were added 15 minutes before IgE stimulation (ie, when these reagents did not significantly increase PER2 levels; Fig 1); (3) PF4800567 did not increase PER2 levels in mast cells and did not affect IgE-mediated allergic reactions (see Fig E7); and (4) PF670462 or corticosterone did not affect cellular viability and baseline cellular bioenergetics of mast cells (see Figs E2 and E3). These findings strongly suggest that PF670462 or corticosterone inhibited IgE/mast cell–mediated allergic reactions depending on the functional mast cell clock (ie, increased PER2 levels), excluding effects unrelated to clock function or other nonspecific effects. This is likely also the case with IgE/basophil-mediated allergic reactions (Fig 5).

The clock-dependent inhibitory effects of PF670462 or corticosterone on IgE-mediated allergic reactions in mast cells were associated with suppression of cell-surface FcεRI expression (Fig 1). The level of mast cell surface FcεRI expression clearly can influence the cell's functional responses to FcεRI-dependent stimulation.[26-29] Thus PF670462 or corticosterone likely suppressed IgE-mediated allergic reactions in mast cells by downregulating FcεRI levels. Because overexpression of PER2 in BMMCs or treatment of BMMCs with a PER2-increasing reagent, aminophylline, also reduced FcεRI expression and signaling (see Figs E9, *A-D*, and E10), whereas *Per2* mutation in BMMCs enhanced FcεRI expression and signaling (se Fig E9, *E* and *F*), it is likely that PF670462- or corticosterone-induced PER2 suppresses FcεRI expression and signaling in mast cells. We have previously shown that CLOCK promotes expression of FcεRIβ, an amplifier of FcεRI expression and signaling,[12] by binding to the E-box–like elements in the promoter region of the gene, thereby temporally regulating FcεRI expression and signaling in mast cells.[11] Thus it is possible that PF670462- or corticosterone-induced PER2 results in suppression of CLOCK activity, thereby repressing FcεRI expression and signaling in mast cells. However, because PER2 can physically interact with different nuclear receptors that might affect FcεRI signaling pathways,[30] the precise mechanisms remain to be determined.

CK1δ and CK1ε play critical roles in the circadian timing system, especially in determining period length, by controlling the rate at which the PER/CRY complexes are either degraded or enter the nucleus.[1-3,8] Initially, both CK1δ and CK1ε were considered important for determining the intrinsic period length in the clock; however, recent studies suggest that CK1δ might play a dominant role in functioning of the circadian timing mechanism.[20,31] The current findings that the pan-CK1δ/ε inhibitor PF670462, but not the specific CK1ε inhibitor PF4800567,

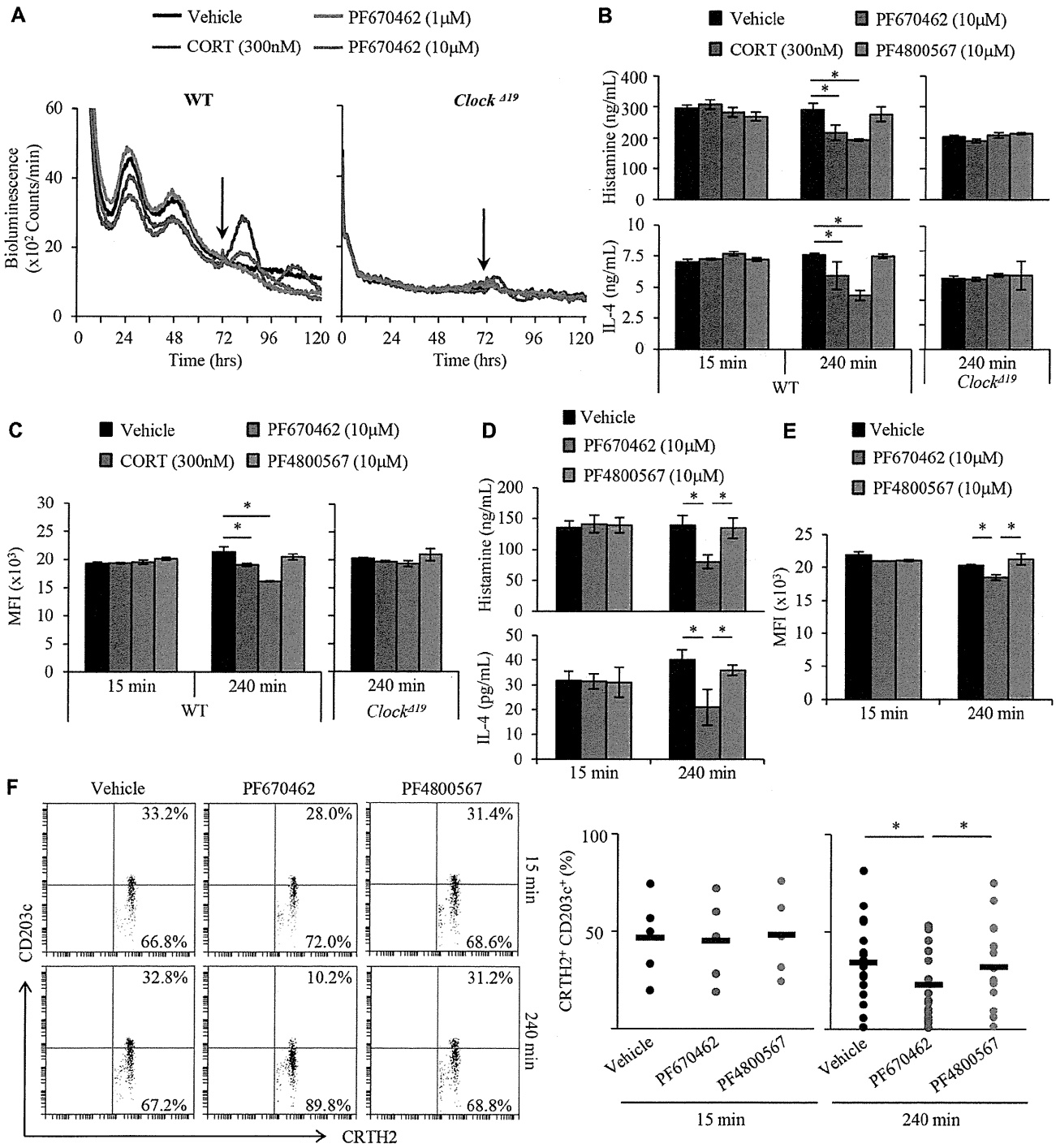

FIG 5. PF670462 or corticosterone suppresses IgE-mediated allergic reactions in mouse and human basophils. **A,** PER2^{LUC} bioluminescence of bone marrow–derived basophils derived from *Per2^{Luc}* knock-in mice (PER2^{LUC} BM basophils) with or without *Clock* mutation (WT or *Clock$^{\Delta 19}$*). PF670462 or corticosterone *(CORT)* was added at 72 hours after the media change, as indicated by *arrows*. **B,** IgE-mediated production of histamine and IL-4 in wild-type or *Clock*-mutated PER2^{LUC} BM basophils (n = 4-6). **C,** FcεRIα levels on wild-type and *Clock*-mutated PER2^{LUC} BM basophils (n = 4). *MFI,* Mean fluorescence intensity. **D,** IgE-mediated histamine or IL-4 production in basophils from peripheral blood of healthy volunteers pretreated with PF670462 or PF4800567 for 15 or 240 minutes (n = 4). **E,** FcεRIα levels on basophils from peripheral blood of healthy volunteers pretreated with PF670462 or PF4800567 for 15 or 240 minutes (n = 3). **F,** CD203c expression on basophils after stimulation with JCP. Basophils were pretreated with 10 μmol/L PF670462 or PF4800567 for 15 (n = 5) or 240 minutes (n = 16) before JCP stimulation. *Left panels,* Representative data; *right panels,* quantitative data. See also Table E1. *CORT,* Corticosterone; *CRTH2,* chemoattractant receptor–homologous molecule expressed on T_H2 lymphocytes; *WT,* wild-type. Values represent means ± SDs. *$P < .05$.